

January 2015

STIRLOCHARGER POWERED BY EXHAUST HEAT FOR HIGH EFFICIENCY COMBUSTION AND ELECTRIC GENERATION

Adhiraj B. Mathur
Purdue University

Follow this and additional works at: https://docs.lib.purdue.edu/open_access_theses

Recommended Citation

Mathur, Adhiraj B., "STIRLOCHARGER POWERED BY EXHAUST HEAT FOR HIGH EFFICIENCY COMBUSTION AND ELECTRIC GENERATION" (2015). *Open Access Theses*. 1153.
https://docs.lib.purdue.edu/open_access_theses/1153

This document has been made available through Purdue e-Pubs, a service of the Purdue University Libraries. Please contact epubs@purdue.edu for additional information.

**PURDUE UNIVERSITY
GRADUATE SCHOOL
Thesis/Dissertation Acceptance**

This is to certify that the thesis/dissertation prepared

By ADHIRAJ MATHUR

Entitled

STIRLOCHARGER POWERED BY EXHAUST HEAT FOR HIGH EFFICIENCY COMBUSTION AND ELECTRIC GENERATION

For the degree of MASTER OF SCIENCE

Is approved by the final examining committee:

DR. HAIYAN ZHANG

Chair

WILLIAM HUTZEL

DR. XUIMIN DIAO

To the best of my knowledge and as understood by the student in the Thesis/Dissertation Agreement, Publication Delay, and Certification Disclaimer (Graduate School Form 32), this thesis/dissertation adheres to the provisions of Purdue University's "Policy of Integrity in Research" and the use of copyright material.

Approved by Major Professor(s): HAIYAN ZHANG

Approved by: DR. DUANE DUNLAP

Head of the Departmental Graduate Program

Date

STIRLOCHARGER POWERED BY EXHAUST HEAT FOR HIGH EFFICIENCY COMBUSTION AND
ELECTRIC GENERATION

A Thesis

Submitted to the Faculty

of

Purdue University

by

Adhiraj B. Mathur

In Partial Fulfillment of the

Requirements for the Degree

of

Master of Science in Mechanical Engineering Technology

December 2015

Purdue University

West Lafayette, Indiana

ACKNOWLEDGEMENTS

I would like to thank my advisor Dr. Henry Zhang, the advisory committee, my family and friends for supporting me through this journey.

TABLE OF CONTENTS

	Page
LIST OF TABLES	vi
LIST OF FIGURES	vii
LIST OF ABBREVIATIONS	xi
ABSTRACT	xiii
CHAPTER 1 INTRODUCTION	1
1.1 Scope	3
1.2 Significance	4
1.3 Research Question	5
1.4 Assumptions	6
1.5 Limitations	6
1.6 Delimitations	7
1.7 Definition of Key Terms	7
1.8 Summary	8
CHAPTER 2 LITERATURE REVIEW	9
2.1 The design, basic working and types of a Stirling Engine	11
2.2 Performance of Stirling Engines	13
2.2.1 Study of torque on a β -type Stirling engine	13
2.2.2 Study of torque and pressure of a Stirling engine	15
2.2.3 Variations of volume with crank angle	18
2.2.4 Study of noise	22
2.2.5 Turbocharger performance in low exhaust environment	24
2.2.6 Heat transfer from the turbine wall to compressor wall	26

	Page
2.2.7	Friction losses in Turbochargers 29
2.2.8	Super Stirling Engine 32
2.2.9	Working fluids for Stirling engines 34
2.2.10	Stirling engine design parameters 35
2.2.11	Stirling engine with a low temperature differential 36
2.2.12	β -Stirling engine with a rhombic drive 37
2.3	Summary 39
CHAPTER 3	RESEARCH METHODOLOGY 41
3.1	Data Collection Methods 41
3.2	Analysis 44
3.3	Threats To Validity 45
CHAPTER 4	RESULTS 46
4.1	β -Stirlocharger 2D Schematic with Variables 46
4.2	Engine to Stirlocharger Relationship 46
4.3	Pressure of Working Gas In Stirlocharger 47
4.4	β -Stirlocharger Power 49
4.5	α -Stirlocharger Power 50
4.6	Compressor Speed of Stirlocharger 50
4.7	Compressor Boost Pressure 51
4.8	Stirlocharger Compressor Mass Flow Rate 52
4.9	Stirlocharger Thermal Efficiency 53
4.10	Response Time of Stirlocharger 54
4.11	Gear Train Analysis 55
4.12	Numerical Simulations 56
4.12.1	β -Stirlocharger 56
4.12.2	α -Stirlocharger 60
CHAPTER 5	SUMMARY, CONCLUSIONS AND RECOMMENDATIONS 64
5.1	MODEL 64
5.1.1	3D Model of the β -Stirlocharger 64

	Page
5.1.2	3D Model of the α -Stirlocharger 66
5.2	MANUFACTURED PROTOTYPE 68
5.2.1	β -Stirlocharger Prototype 68
5.2.2	α -Stirlocharger Prototype 70
5.3	Baseline Tests 71
5.3.1	Torque Test on Compressor Impellor 71
5.4	Turbine Backpressure Measurement Test 72
5.4.1	Turbine without the compressor attached 74
5.4.2	Turbine with the compressor attached 75
5.4.3	Backpressure Test Results 75
5.5	Conclusions 77
5.5.1	Design 77
5.5.2	Performance 80
5.5.3	Conclusion 87
5.6	Recommendations 89
	LIST OF REFERENCES 91
	APPENDIX 94

LIST OF TABLES

Table	Page
<i>Table 2.2-1: Relative heat transfer characteristics for various gases</i> (Thombare, 2006).	35
<i>Table 5-1: β-Stirlocharger Specifications</i>	65
<i>Table 5-2: α-Stirlocharger Specifications</i>	67

LIST OF FIGURES

Figure	Page
<i>Figure 2-1: The β-Stirling Engine Schematic(Foster, 2011)</i>	11
<i>Figure 2-2: The Ideal Stirling cycle (Scollo, 2008)</i>	12
<i>Figure 2-3: Variation of cold Power and Torque as engine speed is increased for heater temperature 350°C of a β-Stirling(Sripakgorn et. al., 2010)</i>	17
<i>Figure 2-4: Variation of cold volume, hot volume, and total volume with crank angle (Karabulet et. al., 2010).</i>	18
<i>Figure 2-5: Variation of brake power with engine speed (Karabulet et. al., 2010)</i>	21
<i>Figure 2-6: Variation of brake power and engine torque with charge pressure (Karabulet et. al., 2010).</i>	21
<i>Figure 2-7: Direction of heat flux in a Turbocharger system (Aghaali, 2013)</i>	28
<i>Figure 2-8: Stirling cycle with single multi-phase working fluid (Gu, 2001)</i>	36
<i>Figure.2-9: Rhombic drive mechanism for a β-Stirling engine (Cheng, 2013)</i>	38
<i>Figure 3-1: Proposed sensor location and Stirlocharger Schematic</i>	42
<i>Figure 4-1: Planetary Gear Train Schematic</i>	55
<i>Figure 4-2: The variation in the hot and cold volumes of the β-Stirlocharger.</i>	56

Figure	Page
Figure 4-3: The pressure of the β -Stirlocharger is shown with respect to the crank angle. The peak pressure is 147.98 kPa.....	57
<i>Figure 4-4</i> : The simulated power of the β -Stirlocharger using the equations described in section 4.2.....	57
Figure 4-5: Simulated Speed of the β -Stirlocharger using the equations in described in section 4.3.....	58
Figure 4-6: Simulated output Boost Pressure of the β -Stirlocharger.	58
Figure 4-7: Simulated mass flow rate of air through the β -Stirlocharger compressor. ...	59
Figure 4-8: Simulated β -Stirlocharger thermal efficiency.....	59
Figure 4-9: The variation in the hot and cold volumes of the α -Stirlocharger.	60
Figure 4-10: The pressure of the α -Stirlocharger is shown with respect to the crank angle. The peak pressure is 2550 kPa.....	60
Figure 4-11: The simulated power of the α -Stirlocharger using the equations described in section 4.2.....	61
Figure 4-12: Simulated Speed of the α -Stirlocharger using the equations in described in section 4.3.....	61
Figure 4-13: Simulated output Boost Pressure of the α -Stirlocharger.	62
Figure 4-14: Simulated mass flow rate of air through the α -Stirlocharger compressor...	62
Figure 4-15: Simulated β -Stirlocharger thermal efficiency.....	63
<i>Figure 5-1</i> : β -Stirlocharger 3D Model Schematic.....	64

Figure	Page
<i>Figure 5-2: α-Stirlocharger 3D Model Schematic.....</i>	66
Figure 5-3: α -Stirlocharger Piston-Cylinder Rotational Schematic. (a) Normal position of the piston-cylinder, piston near pivot. (b) Piston-Cylinder rotates 15° CW as Piston approached TDC. (c) Piston-Cylinder rotates 15° CCW as Piston approached BDC.....	67
<i>Figure 5-4: β-Stirlocharger</i>	68
Figure 5-5: Interior cylinder friction Zone.....	69
<i>Figure 5-6: Force acting on the piston for (a) Stationary condition, (b) Pulling outward condition, (c) Pushing inward condition</i>	69
Figure 5-7: α -Stirlocharger	70
Figure 5-8: α -Stirlocharger Flywheel Pivot.....	71
Figure 5-9: Impellor with Aluminum arm and thread loading.....	72
Figure 5-10: Backpressure Test Bench.....	73
Figure 5-11: Backpressure test schematic without compressor	75
Figure 5-12: Air velocity measurements taken within the exhaust manifold of the test bench.....	76
Figure 5-13: Pressure Differential measurements taken within the exhaust manifold of the test bench	77
Figure 6-1: A comparison of the β and α Stirlocharger output power	80

Figure	Page
<i>Figure 6-2: Increase in the area within the P-V diagram for the Stirlocharger. (a) P-V diagram for β-Stirlocharger at engine speed 100 RPM, (b) P-V diagram for β-Stirlocharger at engine speed 6000 RPM, (c) P-V diagram for α-Stirlocharger at engine speed 100 RPM, (d) P-V diagram for α-Stirlocharger at engine speed 6000 RPM</i>	82
Figure 6-3: Comparison between the Speed of the Stirlocharger for α and β engines....	82
Figure 6-4: Comparison of the boost pressure generated by the α and β engines.....	83
Figure 6-5: IHI RHF4 Compressor Map showing the peak and average dP produced by the α -Stirlocharger	84
Figure 6-6: A comparison of the α and β Stirlocarger compressor mass flow rates.	85
Figure 6-7: A comparison of the thermal efficiencies between the α and β Stirlochargers.	86
Figure 6-8: Comparison of the affect on engine performance between the α and β engine.....	87

LIST OF ABBREVIATIONS

IC	Internal Combustion
EGR	Exhaust Gas Recirculation
η_v	Volumetric Efficiency
CI	Compression Ignition
SI	Spark Ignition
W	Watt
K	Kelvin
J	Joules
rpm	Revolutions per minute
NO _x	Oxides of Nitrogen
TDC	Top Dead Center
BDC	Bottom Dead Center
ICS	Internal Combustion Stirling
WOT	Wide Open Throttle
MEP	Mean Effective Pressure
aTDC	After Top Dead Center
T _H	Heater Temperature

V_{SWC}	Swept Compression Volume
V_{SWE}	Swept Expansion Volume
V_{D}	Total Dead Volume
φ	Phase Angle
N	Engine Speed
LTD	Low Temperature Differential
psi	Pounds Per Square Inch

ABSTRACT

Mathur, Adhiraj MS., Purdue University, December 2015. Stirlocharger Powered By Exhaust Heat for High Efficiency Combustion And Electric Generation. Major Professor: Dr. Haiyan Zhang.

Stirling engines have been in existence since the early 1900s, and have been of little study in the recent years. Stirling engines are low power, heat engines which work on the principle of a temperature differential between the hot and cold sides. This thesis will look into the integration of a Stirling engine onto a turbocompressor for automotive applications calling the device a Stirlocharger.

Some study has been done on the performance characteristics of Stirling engines and turbochargers and is included in this thesis. In a study a Stirling engine was seen to provide a torque of 3 Nm at a hot temperature of 500°C and a cold temperature of 27°C. Torque produced by a conventional turbocharger is in the area of 1.8 Nm. It was also shown that there is significant heat transfer between the hot turbine and the cold compressor. This causes the inlet air to warm up, and reduces volumetric efficiency.

A Stirlocharger would be a promising option to power a turbocompressor, due to its low cost nature, and low noise characteristic. It is also a low maintenance device having lesser complexity parts than a conventional turbocharger.

The α and β Stirlochargers shown in this thesis are potential candidates for automotive use and waste heat recovery applications. The mathematical stirlocharger model presented takes into account the engine speed the device is connected to, and the engine out exhaust gas temperature at varying RPM rates. The engine used for this analysis is a 2L turbocharged Yanmar Diesel engine with a peak power output rating of 50HP. The design and performance comparison between the α and β Stirlochargers is shown and its potential viability for automotive application is assessed. The better candidate is shown to be the α -Stirlocharger. The α and β type Stirlochargers produce boost pressures of 1.75psi and 12.1 psi at 6000rpm respectively, and power outputs of 12.5W and 120.1W respectively.

Upon completing the analysis work mentioned in this thesis, it can be concluded that the Stirlocharger is a potentially strong candidate as an automotive charging system utilizing a waste heat recovery method which can easily be converted into usable torque to propel a compressor.

CHAPTER 1 INTRODUCTION

The Stirling engine was invented by Sir Robert Stirling in 1816, and has been in use since (M.J.Collie, 1979). This engine is a closed cycle air engine, with a hot cylinder side and a cold cylinder side, with no internal combustion, and is also known as an external combustion engine. The hot side can be powered by any heat source, such as an oil lamp flame, a solar concentrator, geothermal, nuclear or biological heat. Stirling engines are capable of producing a relatively good amount of torque for small applications such as water pumping, cryocoolers, heat pumps et cetera. They are usually low power, quiet engines with almost zero emissions. The output capacity of such an engine varies with size, and can be used in automotive applications which are sensitive to size and packaging. Stirling engines have a relatively high efficiency in the order of 40%, with no exhaust gases (M.J. Collie, 1979). This makes it a perfect candidate to be used as a turbocharger coupled to an internal combustion engine.

An example of an internal combustion engine is the Otto cycle engine used in most automotive vehicles these days. An IC engine works on the principles of the Otto cycle, comprising of four strokes namely, intake, compression, power and exhaust. During the intake stroke, a finite volume of air enters the combustion chamber for

compression which leads to combustion. This finite mass of air into the engine is dependent on the ambient temperature and pressure. For colder ambient temperatures the air is more dense therefore, a larger volume can fit into the cylinder, as compared to higher ambient temperatures where less air enters the chamber. The ratio between the mass air flow into the engine, and the cylinder swept volume is known as the volumetric efficiency (η_v) of the engine. The typical volumetric efficiency of a normal IC engine at that open throttle is between 75% - 90% (Pulkrabek, 1997). A turbocharger is a device which forces a higher volume of air into the combustion chamber at normal ambient temperatures, increasing the oxygen content in the chamber for combustion. This has a direct correlation on the amount of torque and power produced. In standard applications, a turbocharger or a supercharger are devices that are employed to apply forced induction during the intake stroke to increase the volumetric efficiency. A turbocharger is a compressor driven by an exhaust gas turbine making use of the exhaust gases from engine. In this device the impeller is driven by the EGR. A supercharger is a similar device, but instead of EGR powering the turbine, the power is drawn from the crankshaft via mechanical linkages. This causes a potential backpressure on the crankshaft which affects the efficiency of the engine. However, the turbocharger is very susceptible to the exhaust gas pressure. For low pressure conditions, the turbo is not very effective and cannot generate enough in cylinder pressures.

In lieu of the turbocharger, a Stirling engine can be used to drive the impeller. The Stirling engine does well in low pressure environments as there is no direct pressure driving any impeller, but just a heat transfer between the EGR and the hot side of the

piston. The small Stirling engine will be attached to the engine housing and in the flow path of the intake manifold. The engine will function as a turbocharger, using the EGR flow and other minute heat transfers from the engine to the hot part of the Stirling. This method is thermodynamically more efficient than just the plain turbocharger, as the exhaust heat is being trapped and used to drive the impeller. This application of the Stirling engine can also be used for other applications such as driving a generator for on vehicle electronics or charging a battery pack for later use.

The main reasons behind using a Stirling engine powered turbo instead of a conventional turbocharger are the greater thermodynamic efficiency, better functionality at low pressure exhaust gasses, higher torque response, better control in transient phases and reduced noise. There is back pressure caused by the turbocharger, which is eliminated with the use of the Stirling engine. The back pressure is caused due to the exhaust gases being pushed back as the flow is constricted by the impeller and nozzle.

1.1 Scope

A Stirlocharger is a Stirling engine powered compressor intake air charger. The main principle behind the new type of device is its waste heat recovery mechanism. A Stirling engine is mounted in parallel with the intake manifold and is connected to a pipe that has engine exhaust gas re-circulating within it. The Stirling engine is a good option to implement due to its higher efficiencies. A direct conversion from heat to electrical energy is very inefficient with cumulative efficiencies on the order of about 28%. The conversion from heat to mechanical energy, which is then converted into electrical

energy, has a much higher conversion efficiency in the order of 70%. The heat transfer medium used in the Stirling engine piston is of critical nature. An optimum working fluid medium needs to be chosen for better heat transfer and compression - expansion of the gas. This will augment the work done by the engine, producing more work with the available exhaust energy. Also an integration strategy needs to be developed to mount the engine onto the engine mount or the engine block. Analysis to find a position optimizing the EGR flow, and power out of the engine will be done. A combination of high density and low density working fluids namely hydrogen (0.0899 kg/m^3), helium (0.1664 kg/m^3), nitrogen (1.20 kg/m^3), argon (1.661 kg/m^3) and carbon dioxide (1.842 kg/m^3) are used within the piston chambers of Stirlocharger and their performance characteristics on the engine efficiency, when exposed to the heat, are studied. The effect of backpressure reduction on NOx emissions will be measured. A comparative analysis between the Stirlocharger and a turbocharger/supercharger will be done to verify the gain in efficiency of the entire system.

1.2 Significance

Common turbochargers today produce power lag and a certain amount of back pressure to the engine (Aggarwal et. al., 2011). A power lag is the time between when the driver presses the accelerator paddle creating a torque request and when the turbo actually produces power. This creates an unexpected jerk while driving. Turbochargers are also generally loud and create noise while running at higher rpm. Using a Stirling engine will eliminate all these issues. They require almost no maintenance due to less number of moving parts compared to a turbocharger. Stirling engines are also very

silent in operation. Also there is no wait time for oil to arrive into the Stirling engine, as compared to in a turbocharger. Turbochargers depend on oil for lubrication and need to wait for oil to arrive once the engine has been turned on. Stirling engine consists of self-contained lubrication and does not require oil to be externally transported. Another key aspect of using a Stirling engine is its versatility. When the Stirlocharger is not in the phase of producing power at full capacity, it can be used to generate power and send it to a battery storage system. Turbochargers, due to their highly detailed geometry, tend to be expensive in the range of \$1000 to \$5000 (turbochargers). The Stirling engine is relatively simple in design, with relatively low cost.

The amount of emissions the engine emits is highly dependent on in-cylinder conditions during the intake stroke. Nitric oxide (NO) formation increases with higher temperatures (Heywood, 1988). By the Otto cycle analysis, for every 10°K change in the intake charge temperature there is a 100°K change in the exhaust gas temperature, corresponding to a factor of 10. The elimination of the backpressure reduces the intake charge temperature by approximately 20°K, causing an exhaust temperature reduction of 200°K which will significantly reduces the NO_x emissions.

The resulting Stirlocharger will be less noisy, and eliminate in-cylinder backpressure to increase engine life in comparison to using a standard turbocharger.

1.3 Research Question

- Is using a Stirling engine powered compressor, the Stirlocharger, a viable option for current automotive applications ?

1.4 Assumptions

The things that could affect the results of the project, but are beyond the researcher's control are,

- The exhaust gas flow rate at the exhaust manifold.
- Adiabatic combustion.
- Exhaust gas energy losses during manifold flow.

1.5 Limitations

- There is no experimental basis for validating the results.
- The Stirlocharger model is ideal.
- The device is not tested on the engine.
- The 3D model is too large and requires further optimization.

The things that will be included and explained in this thesis are,

- The method of using a Stirling engine as a method for engine waste heat recovery.
- The thermodynamic analysis of the Stirlocharger.
- The method of integrating a Stirlocharger to a diesel engine.
- The method of controlling the Stirlocharger using closed loop control.
- The method of split power generation by the Stirlocharger and power storage.

- The definition of the most favorable working fluid to optimize expansion rate of the piston.
- Experimental performance evaluation of the device emphasizing on NOx emissions
- Design of the prototype.
- Stirlocharger's performance at peak engine loads.
- Stirlocharger's performance at low engine speed.

1.6 Delimitations

The things that will not be included in the thesis are,

- Integration with spark ignition (SI) engines.
- Testing of other working fluids with the Stirlocharger except the one being used.
- Analysis of alpha and gamma type sterling engines.
- A secondary turbocharger will not be included.
- Stirlocharger's performance at extreme ambient temperatures.

1.7 Definition of Key Terms

Otto cycle: An ideal air-standard automobile engine cycle.

Stirlocharger: A Stirling engine powered turbocharger.

Turbocharger: A turbine driven forced induction device used to increase the power produced by the engine.

Compressor: A rotary unit which compresses the incoming air to increase flow velocity.

1.8 Summary

Some of the key aspects that will be looked at in this thesis are the method of using a Stirling engine to power a compressor, the optimum working fluid to use in the engine, and a thermodynamic analysis of the Stirlocharger. A design of the prototype Stirlocharger will be used to obtain performance characteristics.

CHAPTER 2 LITERATURE REVIEW

Vehicle manufacturers today are constantly trying to develop new kinds of technologies and engine designs to increase power, and reduce fuel consumption. A common engine in an automobile is of two types: a spark ignition (SI) or a compression ignition (CI) engine. To enhance the power output diesel engines are frequently equipped with a device, commonly known as a turbocharger. The reason why more diesel engines are equipped with turbochargers is due to their ability to sustain high in-cylinder pressures owing to the high compression ratios achieved in the engines. The higher compression ratio engines are more thermally efficient and can therefore accept a higher pressure charge in the intake produced by the turbocharger. The usual thermal efficiency of a diesel engine is in the range of 40-45% (Heywood, 1988).

A turbocharger increases the volumetric efficiency of an engine by forcing more air into the combustion chamber, which is also known as forced induction. A turbocharger is a waste heat recovery system and works on the principle of utilizing the exhaust gas pressure of an engine to power an impeller connected to a compressor which forces high pressure air into the combustion cylinder. A backpressure is generated in the exhaust line as the exhaust gas hits the impeller, which affects the in-cylinder pressure during the exhaust stroke. The friction in the

internal bearings of the turbocharger also account for some loss of energy during the functioning on the turbo.

A new air charging concept which uses a Stirling engine to propel the impeller of the compressor rather than a conventional turbocharger is described in this research. A Stirling engine is a heat engine, which runs on a temperature differential between two cylinders with a working fluid inside. A benefit the Stirling engine provides being used in the Stirlocharger as a replacement to the turbine, is that there will be zero back pressure generated as air exits the tail pipe. This will reduce disturbances in the in-cylinder pressure during the exhaust stroke when the exhaust valve is open, and also reduce the amount of re-circulated residual exhaust gas to enter the chamber. As a result of using a Stirling engine to improve efficiency, the working fluid in the engine also plays a critical role in the working of the Stirlocharger. The working fluid is the medium of energy transfer, and must be optimized to work efficiently to improve the performance of the Stirlocharger. Some research performed by investigators on the working of a Stirling engine and a turbocharger pertaining to its integration onto an IC engine are shown here in a some detail. The effects of using different working fluids in the Stirling engine are also shown here. This will create a preparatory point from which the work in this thesis will be based on.

2.1 The design, basic working and types of a Stirling Engine

A basic Stirling engine design works on the principles of heat exchange between the cold and hot working spaces. A heat source is provided to the hot working space which adds heat to the system. The heating causes the working gas to expand within the cylinder pushing the power piston. The displacer is required to help displace the working fluid between the cold. The region between the displacer and the piston is the cold space region and is kept cooler than the hot space to form a temperature differential. When the hot gas reaches the cold space, it contracts and compresses the piston towards the displacer. The connecting rods of the displacer and the piston are offset by 90° on the flywheel and help in overcoming the dead-point of the piston stroke and to enable displacer reciprocation. A common β -Stirling engine schematic is shown in figure 2.1.

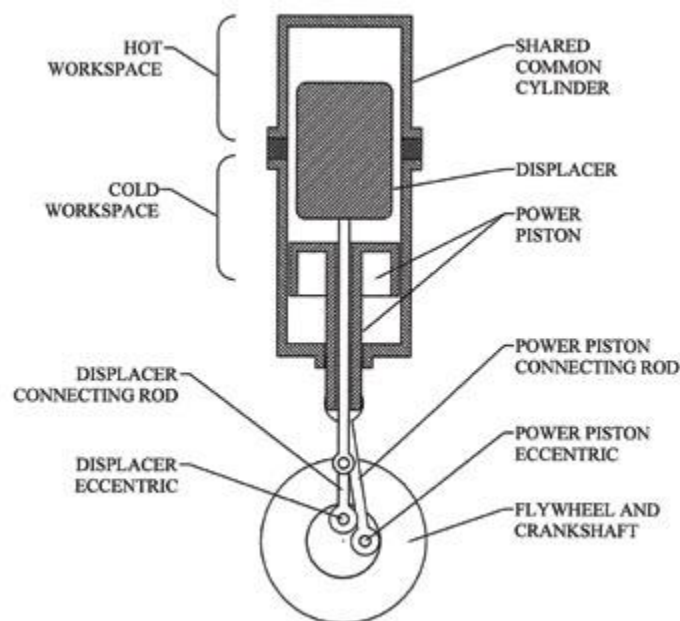


Figure 2-1: The β -Stirling Engine Schematic (Foster, 2011)

The Stirling engine's ideal theoretical cycle is shown in figure 2.2 (Scollo, 2008). Process 1-2 is an isothermal compression stroke. The rejected heat is absorbed in this process by the cold water in the compression exchanger. Process 2-3 is an isochoric process during which the heat is transferred by the regenerator back to the working gas, it is a gas warming process. Heat is absorbed from the heater by the working gas and useful work is done by isothermal expansion during process 3-4. Finally, process 4-1 is isochoric cooling and is the completion of the cycle. Even in Process 4-1 the regenerator helps in heat exchange between the gas. The regenerator is a very important part of the cycle as it absorbs heat in process 4-1 and rejects the heat back during process 2-3. The heat exchanged on these two transformations is up to seven times the heat in processes 1-2 and 3-4 (Scollo, 2008).

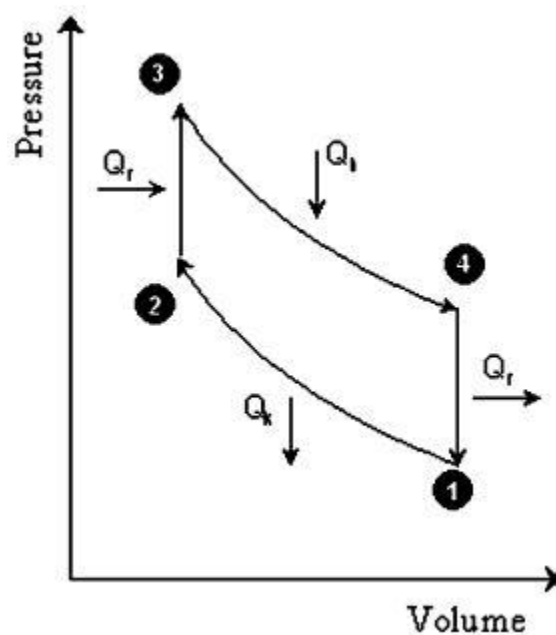


Figure 2-2: The Ideal Stirling cycle (Scollo, 2008)

There are three configurations for Stirling engines namely, the alpha type, beta type, and gamma type. The α -type engine consists of two distinct cylinders, one with the displacer, and the other with the power piston. The power to volume ratio of the α -type engine is high. The β -type configuration is a single axis design, with the displacer on the same plane as the working piston. The gamma type has the power piston mounted in a separate cylinder alongside the displacer piston cylinder but is still connected to the same flywheel. The gamma engine produces lower compression ratio (Karabulut, 2009). In this study a beta type Stirling engine will be used, due to its compactness and easy installation compared to the α -type and gamma type engines which consists of two distinct cylinders respectively.

2.2 Performance of Stirling Engines

The performance of the Stirlocharger device is of key concern in this investigation and is directly related to the performance of the Stirling engine. The torque generated by the Stirling engine is dependent on the heat supplied and the length of the power piston stroke. Some work performed by past investigators are reviewed here.

2.2.1 Study of torque on a β -type Stirling engine

Some work done using beta type Stirling engines are shown here. A study conducted by Karabulut et. al, (2009) used a beta type Stirling engine. In this study two different designs of the displacer cylinder were manufactured and tested. One of them has a smooth inner surface and the other has an enlarged inner surface with rectangular slots having 2 mm width and 3mm depth (Karabulut et al., 2009). Water

circulation is used to cool the external surface of the piston liner. The value of the clearance between the piston and piston liner was determined experimentally. The crankshaft has only one pin for the connection of the piston rod and lever arm. The lever consists of two arms with 70° conjunction angle. The loss of working fluid through the crankshaft bed was prevented by using an oil pool around the crank shaft end-pin. There was no leak for charge pressure below 5 bars. A thermodynamic analysis was conducted using the nodal program presented by Karabulet et al., (2009). The experiments were conducted at 180°C , 200°C and 260°C hot-end temperatures.

For the Stirling engine with helium as a working fluid, the torque increases as the engine speed decreases (Karabulet et al., 2009). Increasing the heat exchange time and decreasing the flow losses, which result in decreasing speed, have positive effects on the torque. The torque also reduces as the working fluid rate of escape increases. The increase in torque terminates at lower speeds due to the prevalence of the negative effects caused by the escaping fluid over the positive effects. There appears to be a more favorable charge pressure at which a higher speed-torque curve is obtained for each value of hot end temperature which is applied to the engine. For 180°C , 220°C and 260°C hot end temperatures optimum charge pressures are 2,3 and 4 bars respectively; maximum torques are 1.33Nm, 2.15Nm and 3.99Nm respectively; the corresponding speeds are 400rpm, 376rpm, 266rpm. The maximum power speed varies with respect to hot end temperatures and the

charge pressures. However, it appears in the range of 500-600 revolutions per minute (Karabulet et al., 2009).

Torque plays an important role in this study, as the new Stirling engine design needs to compete and provide adequate torque to the impeller as a conventional turbine does. This study also shows, that the torque of the engine increases as the speed of the Stirling engine decreases, which can be described by Eq. 2.1 (Pulkrabek, 2003).

$$\tau = \frac{5252 * \dot{W}}{N} \quad (\text{Eqn 2-1})$$

Therefore, as the Stirlocharger's speed is reduced, its torque will increase, and thus at lower power demands the pressure of air into the cylinder will be higher. This is of concern and must be studied in further detail.

2.2.2 Study of torque and pressure of a Stirling engine

In another study conducted by Sripakgorn et al. (2010), to assess the performance, a Stirling engine is connected to a 120W DC generator. A heater is also used to heat the working fluid in the hot piston cylinder region. The generator is coupled with an electronic load in order to adjust the engine accurately. In order to measure the output power from the shaft, the engine is kept on a cradle and is free to rotate. The measurement of the shaft torque is provided by a calibrated torque arm which is attached to the generator. The output power of the shaft can be measured by using the available running speed from the tachometer (Sripakgorn, 2010). The hot end temperature is designed to be between 350°C and 500°C. The maximum power is set to 100W and a charge pressure of 7 bar is maintained. Air

was selected as a working fluid, as hydrogen was a safety concern. The entire mechanism of the Stirling was designed to run without an oil sump. The ratio of the length to bore is 1.35. The space between the displacer and the cylinder liner, the clearance space, is 0.5mm. The heater section is heavily insulated on the outer side ceramic fiber to minimize heat transfer loss due to the environment (Sripakgorn, 2010).

For a heater temperature of 350°C, the engine produces a maximum power of 3.8W under the atmospheric pressure (Sripakgorn, 2010). The maximum power increases with increasing atmospheric pressure and reached a value of 26.6W at 7 bar. For the heater temperature of 500°C, the maximum power was shown to be 95.4W at 360 rpm. The torques for the 350°C and 500°C are 1.77Nm and 2.94Nm at 7 bar respectively. The ratio of the output power by the shaft to the input electrical power into the heater defines the thermal efficiency of the engine, as shown in Eq. 2.2.

$$\eta_t = \frac{(P_s)_{in}}{W_{out}} \quad (\text{Eqn 2-2})$$

The maximum thermal efficiency reached was at 500°C of 9.35%. As the heater temperature was increased, an increase in thermal efficiency was also noticed. The west number¹ was also calculated, and is comparable with the high temperature design (Sripakgorn, 2010). Their study has significant findings in the area of Stirling engines. Current Stirling engine study is being focused on two areas

¹ The west number is an empirical equation used to characterize Stirling engines and other Stirling type engines.

namely, the high temperature and low temperature difference designs. Their study tests the performance of an engine in the moderate to low temperature difference setting. The torque and power output for two different temperatures, 350°C and 500°C, are shown and verified through the west number. Also a low cost design was implemented which corresponds to the low temperature difference (Sripakgorn, 2010).

The power produced at 500°C is 95.4W, at a 360 rpm. The lower heater temperatures produce a lower power output, and is therefore a critical design consideration. The hot core area, must be maintained at over 400°C for the Stirling engine to be able to produce enough power to turn the impellor and generate enough intake pressure. The torque produced at 500°C which is higher than at 350°C is 2.94 N-m. This torque exceeds the requirement to turn the compressor impeller and generate adequate pressure.

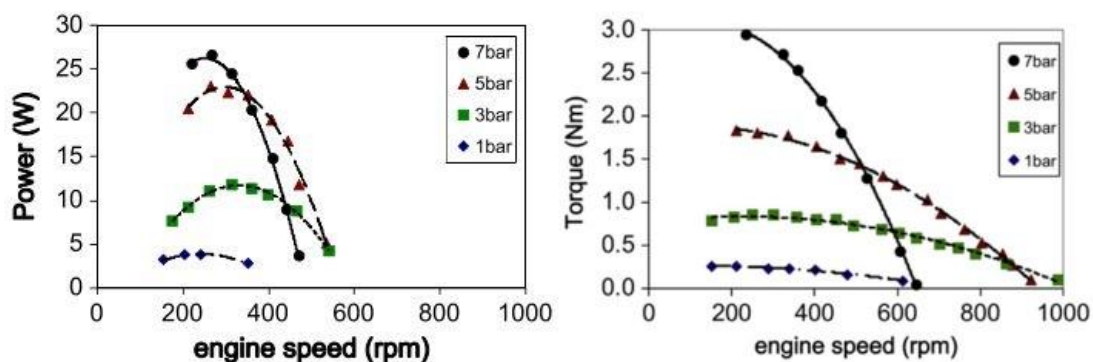


Figure 2-3: Variation of cold Power and Torque as engine speed is increased for heater temperature 350°C of a β -Stirling(Sripakgorn et. al., 2010)

2.2.3 Variations of volume with crank angle

Another study conducted by Karabuletet. al.(2008) shows how the in-cylinder β -Stirling engine volumes and pressure vary with crank angle. The variation of the hot volume, cold volume and the total volume with respect to the crank angle is shown in figure 2.4. The minimum value of the cold volume appears at about 50°CA. This is also the expansion period of the working fluid. The interval of crankshaft angle from 135°CA to 225°CA corresponds to the cooling process at constant volume as the hot volume is constantly decreasing. At 270°CA the hot and total volume are equal as the volume between the displacer and the power piston is zero.

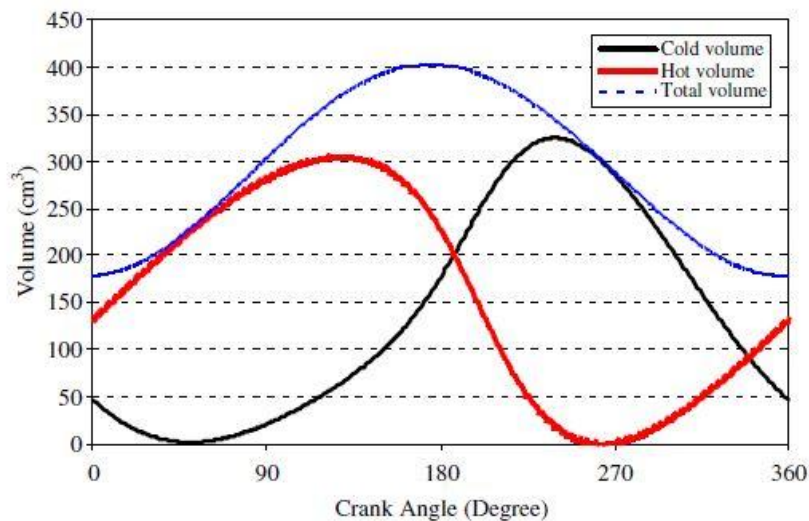


Figure 2-4: Variation of cold volume, hot volume, and total volume with crank angle (Karabulet et. al., 2010).

The engine started to reciprocate at 93°C hot-end temperature, and cooling water temperature of 27°C. The variation of the running temperature of the engine varied up to 125°C for the other tests. Once the heating was stopped, the engine continued to run until the hot-end temperature dropped to 75°C. The variation of

engine power and engine torque with engine speed was shown. The variation of pressure to volume was also shown. These data were obtained at about 200°C hot-end temperature and at different values of charge pressures. The power increases up to a certain level of speed and then decreases. This is estimated due to inadequate heat transfer caused by limited heating and cooling time, and mechanical friction. The power output obtained at 3.5bar and 4.5 bar are lower than 2.8 bar (Karabulet et. al., 2010). Therefore, at 200°C the optimum charge pressure is estimated to be 2.8 bar. The maximum power output at 2.8 bar charge pressure is 51.93 W at 453 rpm engine speed. The brake torque also varies by engine speed. The brake torque also decreases at higher and lower values of speed due to the same reasons which cause the power output to decrease. The maximum values of torque and power occur at almost to the same engine speed.

The convective heat transfer coefficient at the working fluid side of the cylinder, at engine conditions of 2.8 bar charge pressure, 200°C hot-end temperature, 27°C cold-end temperature and 453 rpm, was determined to be 447 W/m²K which corresponded to 51.93 W of shaft power or 6.88 J of shaft work per cycle. To check whether the heat transfer coefficient of 447 W/m²K is valid for other cases, the nodal program was run with 325 rpm engine speed, 1bar charge pressure and 447 W/m²K heat transfer coefficient. The resulting work done was 4.068J. There was a difference in results when compared to the deduced value for work from Fig 2. 5 which came to be 3.32 J. This difference in experimental and theoretical results maybe caused due to mechanical friction which consumes a certain amount of work

produced by the working fluid. The ratio of mechanical losses to the produced work by the working fluid as the engine runs at low power becomes larger. The convective heat transfer coefficient seems to be valid for different situations caused by the engine speed, charge pressure and compression ratio. By equating Nusselt numbers of air and helium the heat transfer coefficient of helium was calculated to be $2392 \text{ W/m}^2 \text{ K}$. With engine conditions of 2.8bar charge pressure, 500C hot-end temperature, 27°C cold-end temperature, 1200 rpm and $2392 \text{ W/m}^2 \text{ K}$ heat transfer coefficient the nodal program predicted an engine power of 493W. The effects of charge pressure to engine power are shown in figure 2.5. As the charge pressure increases, the output power and brake torque increase until a limit, and then decrease. It was also noted that increasing the charge pressure resulted in an increase in vibrations. The slotted cylinder was compared with the smooth cylinder, and it was shown that the slotted cylinders provide 50% more power than the smooth cylinders. This was possible due to low hot end temperature and decrease in the compression ratio (Karabulet et. al., 2010). These results show a promising use of a stirling engine to power a compressor for intake air charging purposes in a vehicle.

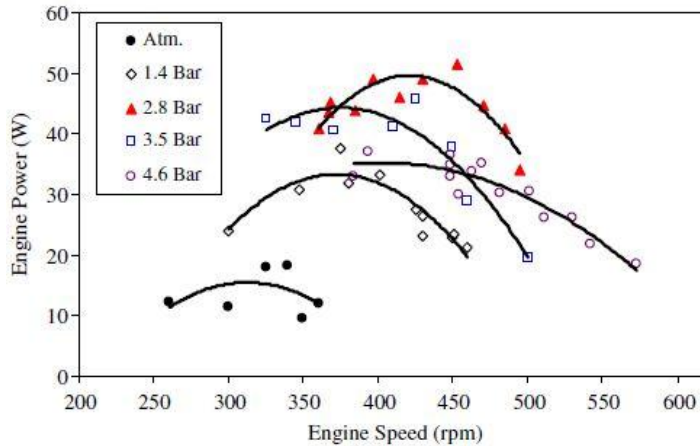


Figure 2-5: Variation of brake power with engine speed (Karabulet et. al., 2010).

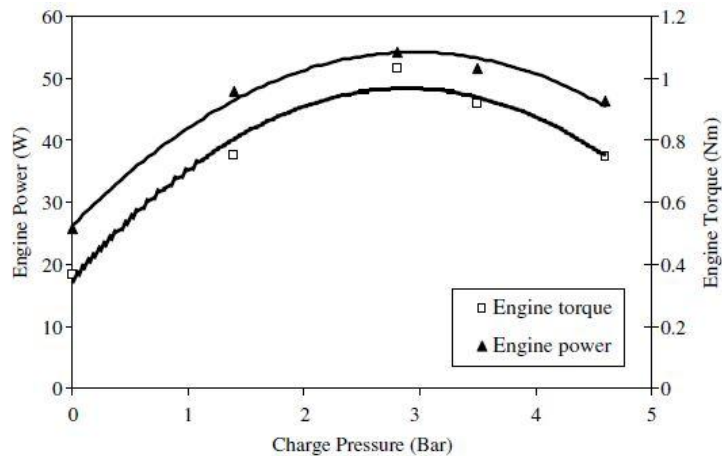


Figure 2-6: Variation of brake power and engine torque with charge pressure (Karabulet et. al., 2010).

If the variation of internal thermal efficiency is examined by the nodal program using a heat transfer coefficient of $447 \text{ W/m}^2 \text{ K}$, charge pressure of 2.8 bar, hot-end temperature of 200C, and cold-end temperature of 27C, a linear relationship can be obtained for engine speed and heat output. The thermal efficiency varies from 12% to 18% as the engine speed varies from 550rpm to 300rpm. As the engine speed increases the experimental and nodal efficiency decrease. It was also shown that as the charge pressure increases the thermal

efficiency of the engine also increases. An efficiency of 20.6% was obtained corresponding to 3.32J of shaft work at ambient pressure. The maximum torque of 1.17 Nm was obtained at 2.8 bar charge pressure (Karabulet et. al., 2010).

It's shown that the pressure of 2.8 bar provides the highest engine power and torque at 453 rpm, and higher pressures do not increase engine power. A pressure of 2.8 bar must be maintained in the Stirlocharger for all operating conditions for optimum performance.

2.2.4 Study of noise

The noise generated by a turbocharger is also of concern as they are loud and produce significant vibrations. Literature on this needs to be reviewed to know better which aspects of the turbocharger produce vibrations and sound, and compare it with Stirling engine. The following study provides an overview of turbocharger noise and vibrations.

A study conducted by Rammalet. et. al., (2007) gives some insight on turbocharger noise and how it is produced. Turbocharger noise is increasingly becoming an issue. The engines are reducing in size due to new imposed laws for emissions, and the easiest solution for that is adding a turbocharger to the system. In turbochargers, both the turbine and the compressor have an influence on how low frequency engine pulsations propagate in the intake/exhaust system, this is called the passive acoustic property of the turbo unit. A turbo unit will also produce high frequency aerodynamic sound, which is referred to as its active acoustic property. The sound is due to the rotating blade pressures, and in modern turbo

units which have supersonic tip speeds producing rotating shockwaves (Rammal, 2007).

The main noise problems seem to be associated with the turbo-compressor outlet side (Rammal, 2007). The new turbochargers normally reach design rotor blade speeds of supersonic flow, and the noise is mainly contributed by the blade passing tonal noise and the buzz-saw noise. The higher the rotor speed, the more prominent the blade passing noise and its harmonics are. The buzz-saw noise typically occurs at high engine power operating conditions and only exists on the inlet side for radial compressors. At lower, subsonic, rotor speeds narrow-band noise components related to rotating instabilities and reversed flow conditions, are found to dominate with peak around half the blade passing frequency. This concludes that at higher engine RPMs the noise is much higher than at low RPMs (Rammal, 2007).

A Stirling engine is known to be relatively silent, and does not generate much vibration. The reason they are relatively silent is because there is no combustion taking place inside the engine. This is known as an external combustion engine, the heat source to power the cylinder at the hot end is externally provided. In the automotive application, when using the exhaust gas to provide heat energy to the hot end of the Stirling engine, there would be no noise produced as the exhaust passing around the hot piston cylinder end is smooth and noiseless.

Low pressure exhaust is of concern for turbocharging applications. The pressure of EGR is critical and has a threshold value at which the impellor starts to

rotate. This pressure needs to be attained before the turbocharger can function optimally. Some investigation done in the low pressure EGR applications of turbocharging is shown here.

2.2.5 Turbocharger performance in low exhaust environment

A study conducted by Gorelet. al., (2001) gives information on the performance of low pressure EGR on turbochargers. Low pressure EGR is more suitable for the engine. To overcome the insufficient differential pressure problem a so called high pressure EGR system is developed. This system re-circulates exhaust gas between the two high-pressure points, namely the turbine inlet and compressor outlet downstream of the intercooler. Small differential pressure naturally exists across the EGR loop but needs to be artificially enhanced to allow for substantial EGR rates, which is typically achieved through de-rating of the conventional turbocharger or use of variable geometry turbochargers. Engines equipped with high pressure EGR system usually suffer durability problems caused by the dirty exhaust being re-circulated into the engine. For maximum NO_x removal the cooling of the EGR gas is required. However, if the EGR is cooled below its dew point, moisture will condense on the EGR loop. This moisture will then react with nitrogen oxides and sulfates forming nitric and sulfuric acids. These acids, along with the condensed water, have a detrimental effect on the metal components of the engine (Gorel, 2001).

This study was done to develop an EGR system suitable for retrofit applications for low pressure applications (Gorel, 2001). One of the features of this

device is a condenser for water removal. The condensed acidic water accumulates at the bottom of the intercooler, and increases resistance to the airflow. If this water is not removed it may enter the engine causing dilution of the lubricating oil and corrosion of internal metal surfaces. During the course of this program the condensed water samples were collected from the bottom of the intercooler. The samples were taken at random time intervals without reference to the test conditions or a specific system configuration. A total of 10 samples were taken and analyzed over the 65 hour testing period resulting at an average condensed water accumulation rate of 10.16 ml/hr. The analysis clearly indicated an acidic environment of the samples with pH level ranging from 3.1 to 4.5. Nitrate and sulfate in the form of nitric and sulfuric acids were also found. The accumulation of sulfates depends on the sulfur content of the fuel and can be substantially reduced by using ultra low sulfur fuel (Gorel, 2001).

The influence of EGR is seen in the increased intake mixture temperature as measured at the compressor inlet (Gorel, 2001). Compressor inlet temperature with EGR is increased by 25-30°C while running at the test cell temperature of about 25°C. The peak temperatures were in the range of 50-60°C. The permitted limit is around 70°C, because higher temperatures may result in the compressor failure. In a real application, such a limit can be exceeded if the ambient air temperature reaches 40-50°C. This condition would cause a substantial loss of power and may result in engine failure. In order to minimize deterioration of the engine's performance and maximize NO_x reduction, one should strive achieve no increase in the inlet

temperature via effective cooling of the EGR stream. As the compressor inlet temperature increases, the boost air temperature also increases exceeding 180°C at speeds above 1350 rpm. The turbo inlet temperature was also increased by application of EGR to a maximum of 674°C (Gorel, 2001).

From this study on low pressure EGR it can be seen that a threshold temperature must be maintained to reduce the condensation of the EGR flow onto the pipe, and to reduce nitric acid formation which can be corrosive to the internal components. The inlet temperature of the compressor must be maintained below 70°C to be safe.

As shown above, the compressor inlet temperature is critical in the safety of the compressor components and has an upper bound of about 75°C . The raise in compressor inlet temperature can be due to a number of reasons such as, ambient air temperature and heat transfer between the hot turbo and the compressor walls. The inlet temperature of the turbo is in the range of around 674°C , which radiates heat to the surrounding components through the walls. Some of this reradiated heat is absorbed by the walls of the compressor, warming up the incoming air. A study done by Aghaali, (2013), shows how the heat released by the turbo affects the turbocharger.

2.2.6 Heat transfer from the turbine wall to compressor wall

A turbocharger is employed to increase the density of the air introduced in the cylinder of an engine. This increases the specific power of the engine thus allowing engine downsizing. Turbochargers always work at high temperatures, and

heat transfer becomes a key concern. The temperatures of the turbocharger walls can influence both the air temperature through the compressor and the exhaust gas temperature through the turbine. This study will show experimentally that turbocharger working fluids are influenced by the temperatures of turbocharger walls as well as turbocharger load point. A research mentioned in the paper concludes that the heat transfer direction can be altered from turbocharger walls to the working fluid of the compressor depending on the turbocharger load point. The compressor impellor temperature vary proportionally to the compressor outlet temperature and the effects of lubricant oil and turbine inlet temperature are relatively minor. Additionally the bearing housing wall temperature varies consistently with the oil temperature in an oil cooled turbocharger. The transfer of heat to the compressor is primarily induced by the bearing housing oil temperature and not directly due to the hot exhaust entering the turbine inlet (Aghaali, 2013).

The engine used for this work was a direct injected 2 liter gasoline engine with a water-oil-cooled turbocharger with a closed waste-gate (Aghaali, 2013). In addition to the base parameters of a turbocharged engine, the parameters that were measured on the turbocharger include the mass flow, fuel flow, turbocharger speed, turbine inlet and outlet pressures, compressor inlet and outlet pressures, turbine inlet and outlet gas temperatures, compressor inlet and outlet air temperatures, the mass flows of the water and oil into the bearing housing of the turbocharger and the inlet and outlet temperature of the water and oil. Three average temperature measurements of the walls were made using thermocouples,

for three main components of the turbocharger, the compressor scroll and back, the turbine housing and back, and the turbocharger bearing housing. Some of the strategies to change the heat transfer mechanism were, using aluminum foil as a radiation shield between the turbine and compressor to avoid radiative transfer of heat from the hot turbine to the compressor, an extra cooling fan was placed over the turbocharger to change the rate of convective heat transfer, insulator was placed on the turbocharger surface to insulate them, and a wide radiation shield was used between the exhaust manifold of the engine and the turbocharger to avoid radiative transfer of heat from the exhaust manifold to the compressor. A schematic showing the heat and energy fluxes on a turbocharger system is shown in Fig. 2.7 (Aghaali, 2013).

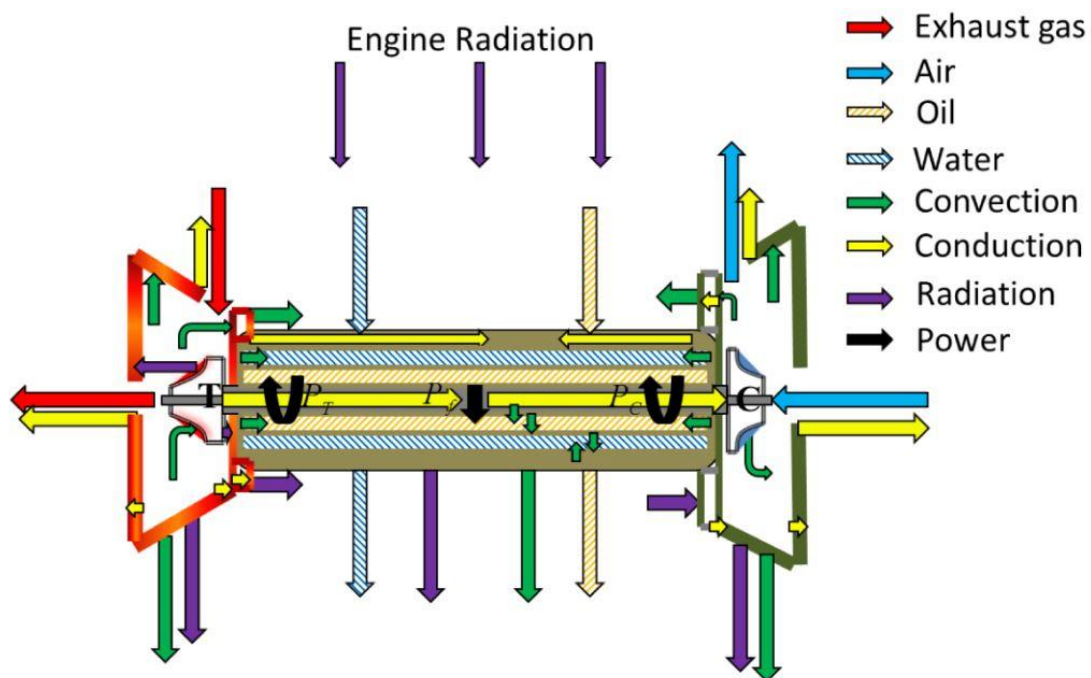


Figure 2-7: Direction of heat flux in a Turbocharger system (Aghaali, 2013)

In conclusion the temperatures of turbocharger working fluids are affected not only by the turbine and the compressor performance but also by the momentary temperatures of the turbocharger walls (Aghaali, 2013). The compressor outlet temperature is a function of the compressor pressure ratio, the temperatures of the compressor walls and the compressor inlet temperature. The turbine outlet temperature correlates closely with the turbine pressure ratio, the turbine inlet temperature, the average temperature of the turbine walls, the bearing housing temperature and the ambient temperature. The temperatures of the turbocharger walls are predictable. The bearing housing temperature and the turbine wall temperature affect the compressor wall temperature. The bearing housing temperature is governed by the cooling water inlet temperature. Lastly, in spite of the fact that the temperatures of the turbine walls are strongly correlated with the turbine inlet temperature, changing the convection condition on the turbocharger can significantly alter the temperatures of the turbine walls (Aghaali, 2013).

2.2.7 Friction losses in Turbochargers

A lot of losses that take place within a turbocharger, are due to friction losses in the bearings. This should be looked into, as the Stirlocharger has significantly fewer components and can help in reducing frictional losses to increase efficiency. Some work done by Serrano, et. al. (2013) shows the affects of friction losses in turbochargers and how to measure them.

The turbochargers being produced currently consist of oil bearings, two journal bearings which support shaft rotation and one double acting axial thrust

bearing which carries the axial load produced due to the imbalance of force between the compressor inducer and the turbine wheel. Most of the mechanical frictional losses occur due to the presence of these bearings in the turbocharger which directly amount for the mechanical efficiency of the turbocharger. The three ways to measure mechanical frictional losses of a turbocharger are (Serrano, 2013):

- Measuring the oil enthalpy variation,
- Measuring the enthalpy of variation of the gas,
- Measuring the friction torque with a rotating torquemeter.

No exchange of heat within the turbocharger, is the assumption required to evaluate the first method, and also the power generated by mechanical friction is totally dissipated by the oil flow (Serrano, 2013). To minimize the heat lost by convection, the entire turbocharger is adequately insulated and the compressor, turbine and central housing are fed with both the air and the oil at a matching temperature. The power due to friction is equal to: (Serrano, 2013)

$$P_{friction} = P_{oil} = q_{m-oil} * c_{p-oil} * (T_{2-oil} - T_{1-oil}) \quad (\text{Eqn 2.1})$$

For the second method it is assumed that the expansion of gas within the turbine and the compressor is adiabatic, i.e. no heat is lost during the expansion due to the instantaneous nature of the occurrence. Here the power of mechanical frictional losses is the difference of the turbine power and the compressor power as shown below: (Serrano, 2013)

$$P_{turbine} = q_{m-turbine} * c_{p-air} * (T_3 - T)_4 \quad (\text{Eqn 2.2})$$

$$P_{compressor} = q_{m-compressor} * c_{p-air} * (T_2 - T)_1 \quad (\text{Eqn 2.3})$$

$$P_{friction} = P_{turbine} - P_{compressor} \quad (\text{Eqn 2.4})$$

For the third method, a rotating torque meter is mounted between the turbine and the central housing containing the bearings (Serrano, 2013). The friction torque generated by the bearings is measured by the torquemeter. It was shown by Podevin et. al. that mechanical efficiency of the turbocharger is strongly dependant on its operating parameters such as rotational speed, oil inlet temperature and inlet oil pressure. The losses due to friction depend on the oil type, oil temperature and oil pressure, and these losses also affect the performance of the turbochargers. The results show that when the applied axial force on the bearings is increased, the losses due to friction rise. The increase in absolute friction power is weak and is between 15.8W and 29.9W. The relative increase in the power lost due to friction is between 4.81% and 11.83% of total friction power. Although the variations in absolute friction losses are weak, the results show that this variation is relatively greater for low rotational speeds. Within the rotational speed zone, the mechanical efficiency is reduced by 1% or 2% if the frictional losses are increased. The power generated by friction is increased by raising the oil inlet pressure (Serrano, 2013).

As can be seen from the above study, there is considerable frictional losses in the operation of a turbocharger. There are fewer components in the Stirling engine, and will therefore, have considerably less frictional losses due to bearings.

A Stirling engine's power can be increased by using high temperature steam or compressed air. This type of Stirling engine is known as a super Stirling. Some

performance characteristics of this type of engine is shown in the study conducted by Isshiki et. al., (1999).

2.2.8 Super Stirling Engine

A super Stirling engine is a type of Stirling which is helped by steam or compressed air injection and ejection. At the TDC of the power piston, steam is injected into the cold side of the displacer piston and then the injected steam goes past the heat regenerator installed in the displacer piston (Isshiki, 1999). The steam is then heated by the heater of the Stirling engine and expands at constant high temperature. At the BDC of the power piston the steam begins to be ejected out to the exhaust pipe by the rotation of rotary valve which changes steam the route to outside. At this steam ejection process, steam passes the heat regenerator in the opposite direction, so the steam goes out at low temperature just the same as a conventional Stirling engine. This can be applied to the β -type Stirling engine, but a larger amount of steam is required. Some of the conclusions were, that the power and speed increases up to several times of conventional Stirling engines, it uses steam instead of helium which is ecologically good, the thermal efficiency of this engine is lower than single Stirling cycle engines and it requires a boiler system to generate steam (Isshiki, 1999).

An engine combination of the Stirling engine with an internal combustion has also been developed and has been studied by Patton et. al. (2011). The engine is a split cycle configuration with a regenerator between the intake/compression cylinder and the power/exhaust cylinder. The regenerator acts as a counter-flow

heat exchanger. During the exhaust, the hot gas is cooled by the regenerator, and is stored. In the next cycle, compressed gases flow in the opposite direction and are heated by the regenerator. The gases coming from the regenerator are very hot ($\sim 900^{\circ}\text{C}$) which provides the necessary gas temperature for auto ignition of the diesel or other fuel (Patton, 2011). The IC engine indicated efficiency increases with increasing compression ratio and is insensitive to peak temperatures, whereas in the ICS engine indicated efficiency increases with decreasing compression ratio and increasing peak temperature. Important ICS engine innovations include elimination of throttling losses, low friction due to low compression ratio, and very high air cycle efficiencies ($\sim 80\%$).

The ICS engine has nearly constant pressure combustion which should help in NO_x reduction. At WOT ICS is more efficient than either a gasoline or a diesel engine. Some of the drawbacks of ICS are the starting, control, power density and combustion uncertainty. The prototype engine is equipped with an intake heater, a cylinder heater and a spark plug for ignition if required. A starting charge needs to be developed to start the engine (Patton, 2011). The control aspect is also crucial as the F/A ratio cannot be too low or the gases will not be hot enough to fire the engine. On the other hand, the F/A ratio cannot be too high or the power valve and regenerator will be damaged due to high exhaust temperatures. The engine has lower power density. Between the low fuel ratio needed to prevent overheating of the valves, and the poor volumetric efficiency due to the dead spaces, the engine does not generate a large amount of power. The WOT has a MEP of approximately

2.6 bar (38psi). This is almost doubled for diesel engines. Also there is combustion uncertainty, the engine fires very late (50° aTDC) and it may have a problem firing, particularly if the engine is not warmed up. It is estimated that the ICS engine under road load conditions will be 50% more efficient than a diesel engine and 75% more efficient than a gasoline engine (Patton, 2011).

2.2.9 Working fluids for Stirling engines

Any high specific heat capacity working fluids may be used for Stirling engines (Thombare, 2006). Most 19th century engines used air as a working fluid, and operated at close to atmospheric pressure. At that time air was cheap and available readily. The following thermodynamic, heat transfer and gas dynamic properties should be exhibited by the working fluids used within a Stirling engine: (Thombare, 2006):

- High thermal conductivity
- High specific heat capacity
- Low viscosity
- Low density

The capability of the working fluid is defined by the capability factor (Thombare, 2006):

$$Capability\ Factor = \frac{thermalconductivity}{specifice\ atcapacity * density} \quad (Eqn\ 2.5)$$

In table 2.1 various fluids are compared using the capability factor and heat transfer at the average temperature and pressure of 800K and 5MPa.

Table 2.2-1: Relative heat transfer characteristics for various gases (Thombare, 2006)

Working fluid	Heat transfer	Capability factor
Air	1.0	1.0
Helium	1.42	0.83
Hydrogen	3.42	0.68
Water	1.95	0.39
Sodium-Potassium eutectic	32.62	1.32

From the table above the only working fluid which satisfied both the requirements is NaK eutectic. University of California San Diego is currently investigating the feasibility of this working fluid.

2.2.10 Stirling engine design parameters

The basic design parameters of the Stirling engine are (Invernizzi, 2010):

- The minimum operating temperature T_K , at the cooler, and the hot temperature T_H at the heater,
- The swept compression volume V_{SWC} and the swept expansion volume V_{SWE} .
- The total dead volume V_D ,
- The phase angle ϕ of the expansion space volume variations relative to the compression space volume variations,
- The speed of the engine N .

The Stirling cycle with single multi-phase working fluid is composed of the following processes corresponding to figure 2.8 (Gu, 2001),

Process 4-1: adiabatic expansion in expansion space for work output,

Process 1-1' and 2-3': heat recovery in heat exchanger,

Process 1'-2: heat rejection to the external dump in condenser with the condensing process,

Process 2-2': pressure lift of the condensed liquid by feed pump,

Process 3-4': heat addition in heater from the external heat source.

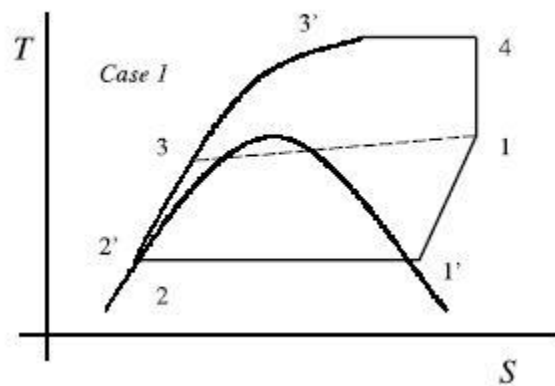


Figure 2-8: Stirling cycle with single multi-phase working fluid (Gu, 2001)

2.2.11 Stirling engine with a low temperature differential

Temperature differential is a critical aspect in the working of a Stirling engine.

The main principle behind the working of a Stirling engine is the temperature differential between the cold and hot piston regions. Therefore, a look into low temperature differential situations, and how the low temperature differential affects engine performance is necessary. A study conducted by Kongtragool, (2006) shows the affects of the performance of a Stirling engine subject to low temperature.

Low temperature differential Stirling engines do exist usually in the gamma configuration without a regenerator (Kongtragool, 2006). It is a type of Stirling

engine that can operate with a low-temperature heat source such as solar energy without magnification. The temperature differential between the hot volume and cold volume can be as low as 100°C. Some characteristics of the LTD Stirling engines are (Kongtragool, 2006),

- Large ratio compression ratio, the ratio between the displacer and power piston swept volumes,
- Large displacer cylinder and displacer diameters,
- Short displacer length,
- Both end plates of the displacer cylinder have large effective heat transfer surfaces,
- Small stroke of the displacer,
- The end of displacer stroke dwell period is rather longer than the normal Stirling engine,
- Operating speed is low.

Due to the temperatures and temperature differential being small, the energy is not sufficient for high power and speed applications. Therefore, LTD Stirling engines are used for low power and speed applications such as water pumping using unmagnified sunlight.

2.2.12 β -Stirling engine with a rhombic drive

A type of Stirling engine which incorporates a rhombic drive is also studied. A rhombic drive is a twin output mechanism with two drives instead of the conventional one. The schematic of this type of engine is shown in figure 2.9. The

rhombic drive was studied by Cheng. et. al. (2013), and its performance characteristics are shown here.

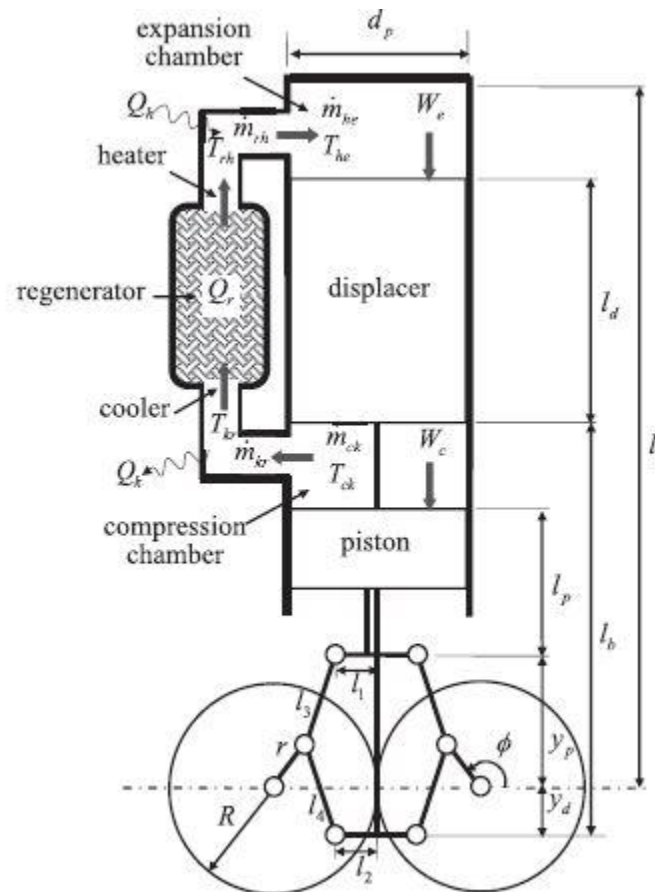


Figure.2-9: Rhombic drive mechanism for a β -Stirling engine (Cheng, 2013)

In this study a domestic scale 300W Stirling engine with rhombic drive mechanism was developed and tested. Experiments were conducted to test the performance of the engine under various operating conditions. Dependence of the shaft power output on the engine speed is investigated under different combinations of working gas, charged pressure, heating temperature, and regenerator wire mesh number. A theoretical model was also build and applied to predict the performance of the engine. Results show that the shaft power output of

the engine is much higher using helium as the working fluid than using air.

Furthermore, as the charged pressure and the heating temperature are set at 8bar and 850°C, and a number 120 wire mesh is used in the regenerator, the shaft power of the engine can reach 390 W at 1400 rpm with 1.21 kW input heat transfer rate, which results in a thermal efficiency of 32.2%. The experimental data were compared with the numerical predictions to verify the theoretical model. It was found that the numerical predictions of the shaft power are higher than the experimental data by 12% - 20% (Cheng, 2013).

2.3 Summary

After investigating a number of factors relating to turbocharger performance and Stirling engines, incorporating a Stirling engine to a compressor in lieu of a turbocharger is shown to have a potential success. There are significant efficiency increases in using a Stirling engine coupled to a compressor. Some of the expectations are:

- Fewer frictional losses
- Less noise and vibrations,
- Increased engine efficiency due to higher energy retrieval from the EGR
- Better performance in low engine exhaust pressure/load conditions.
- Reduced NO_x emissions as a result of lower backpressure while using a Stirlocharger.

The Stirlocharger is a new promising engine waste energy harvesting concept which can deliver better performance in low engine speed situations and reduce cost in manufacturing owing to its simplistic design.

CHAPTER 3 RESEARCH METHODOLOGY

The design, integration and data acquisition of a Stirlocharger onto a diesel engine is more of a design based research approach with limited MATLAB based numerical predictions for Stirlocharger performance.

3.1 Data Collection Methods

After integrating the Stirlocharger onto a diesel engine to initiate forced induction, various measurements need to be taken to demonstrate its functionality, stability and control. The variables to be measured are, exhaust temperature, mass flow rate of exhaust, pressure and rotational speed of the Stirlocharger. The temperature is measured before and after the Stirling heating tube to analyze the work done by the Stirling engine and to show the loss in exhaust temperature which will be used to compute the heat transfer between the exhaust and the Stirlocharger. The engine out temperature and mass flow rate is measured to verify the maximum possible heat energy available for waste energy harvesting. To evaluate the performance of the Stirlocharger, the boost pressure produced by the compressor is measured using a pressure transducer at the compressor outlet. The air inlet temperature of the compressor is also measured using a thermocouple. The air inlet temperature affects

the boost pressure and the volumetric efficiency of the engine. A schematic plan of proposed sensor position is shown in Fig. 3.1.

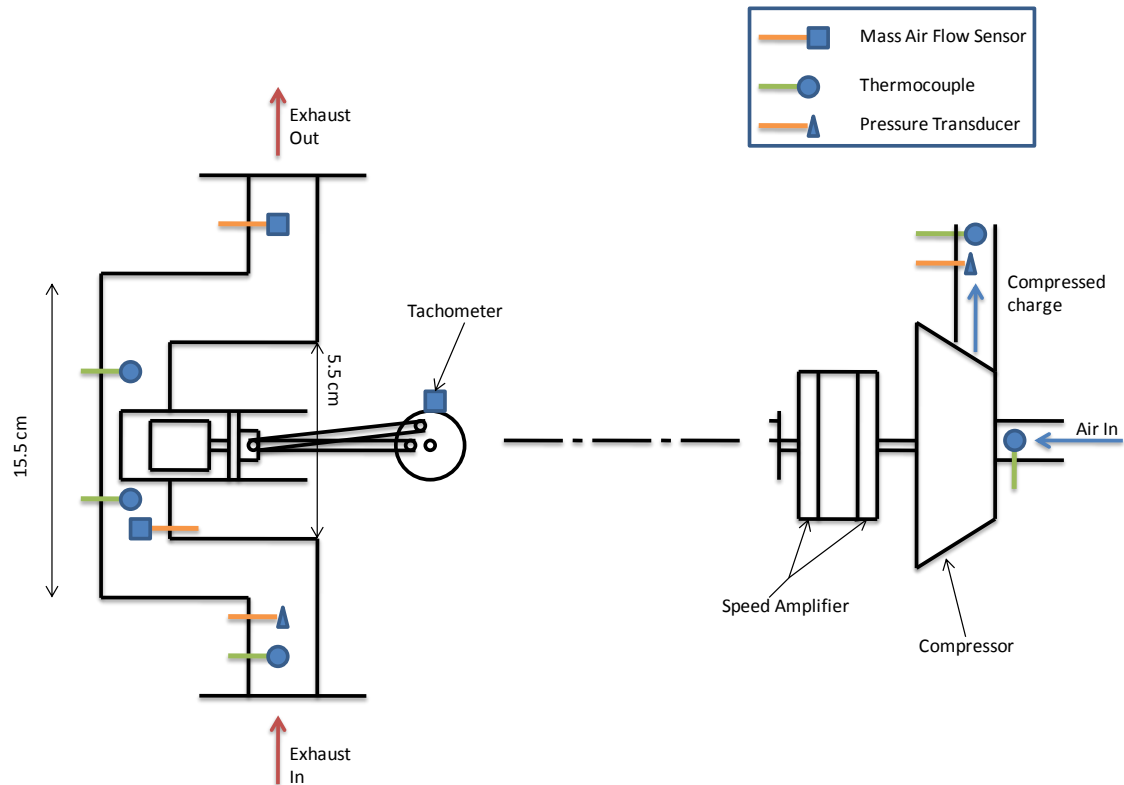


Figure 3-1: Proposed sensor location and Stirlocharger Schematic

All of these measurements are critical in nature to monitor the system while functioning. The data collection equipment required are as follows:

- 5 thermocouples
- 2 Pressure transducers
- 2 mass air flow sensors
- A data logger
- 1 Tachometer
- Dynamometer

The data to be collected is taken at specific intervals. The tachometer is attached to the output shaft of the Stirlocharger to measure the shaft speed in revolutions per second.

To measure the temperature of the working gas in the displacer piston, a hole is machined in the hot area displacer cylinder area and the cold piston area for a thermocouple to be placed. This thermocouple is installed to measure the peak temperature attained in the displacer cylinder and the minimum temperature attained in the cold region. There is also a thermocouple placed in the cylinder of the engine to measure the engine-in-cylinder temperature, to see the effects of the Stirlocharger. To measure pressure, pressure transducers are used. One transducer is placed in the displacer piston to measure the maximum pressure attained in the compression stroke. Another pressure measurement is needed in the engine-in-cylinder to measure the pressure differences with the Stirlocharger switched on and off. This will show the boost generated by the charger, and if it is adequate. The pressure difference between the inlet and outlet of the compressor is also required, to understand the pressure difference the Stirlocharger is generating. This pressure difference will then be compared with a standard differential pressure of a turbocharger of about 3-4 psi. The exhaust mass air flow is also required to be measured. The mass air flow is important for a number of reasons such as, it can quantify a heat transfer rate and give us a data point for how fast should the Stirlocharger run. This will be measured using a mass air flow sensor connected to the exhaust manifold. All the measurements will be compared to predicted values from the theory.

List of variables to be measured and their units:

$$\text{Volumetric Flow rate} - \frac{m^3}{s}$$

$$\text{Temperature} - ^\circ\text{C}$$

$$\text{Pressure} - \text{kPa}$$

Stirling Engine Speed - Revolutions/Second

3.2 Analysis

The data will be analyzed with reference to theoretical computations. A Stirling engine model will be made, and all the pressure values from the cylinder, intake, and exhaust flow will be verified with the experimental data. The interface of the Stirling engine with the intake manifold needs to be optimized for reduced exhaust heat escape. The interface is of critical concern as it must be air tight, and water tight. No debris must enter through the seals. The compressor will be integrated to the Stirling engine.

The work of the Stirlocharger is quantized by the following relationship:

$$W_{\text{Stirlocharger}} = W_{in} + W_{out} - W_{\text{shaftfriction}} \quad (\text{Eqn: 3.1})$$

$$W_{\text{Stirlocharger}} = \left[n * R * T_c * \ln\left(\frac{V_2}{V_1}\right) \right] + \left[n * R * T_h * \ln\left(\frac{V_1}{V_2}\right) \right] - \frac{\dot{m}_c c_{p,a} (T_2 - T_1)}{\eta_c \eta_T \dot{m}_T c_{p,g} T_3 \left[1 - \left(\frac{p_4}{p_3}\right)^{\left(\frac{K-1}{K}\right)_k} \right]} \quad (\text{Eqn: 3.2})$$

Where, n = number of moles

R = Ideal gas constant

T_c, T_h = Temperature of the cold and hot side of the Stirling Engine respectively

V_2, V_1 = Volumes of the cold and hot side respectively

\dot{m}_c, \dot{m}_T = mass flow rate through the compressor and turbine respectively

$c_{p,a}, c_{p,g}$ = coefficient of specific heat

T_1, T_2 = Temperature of the turbine and compressor respectively

η_C, η_T = Compressor and Turbine efficiency respectively

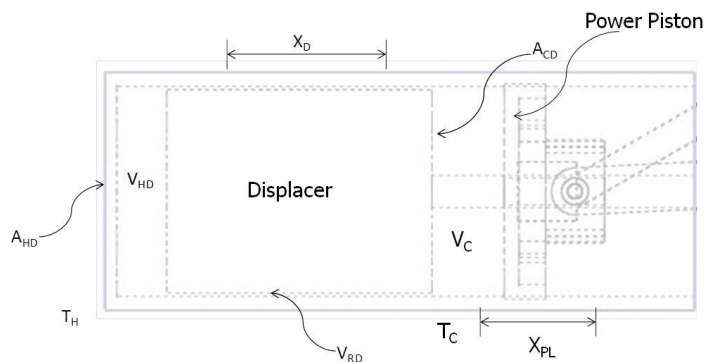
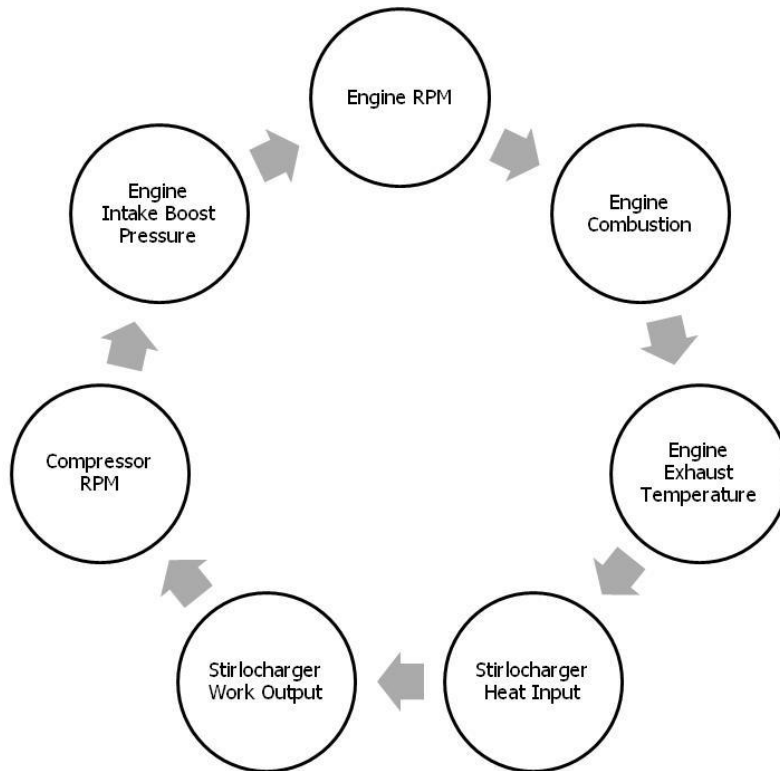
p_4, p_3 = Pressure through the compressor and turbine respectively

$K = c_p/c_v$

3.3 Threats To Validity

- A complete theoretical modeling approach.
- Engine calibration parameters not known.
- Engine cycle-to-cycle variation.
- The exhaust gas temperature data is from a different 2L diesel engine.

CHAPTER 4 RESULTS

4.1 β -Stirlocharger 2D Schematic with Variables4.2 Engine to Stirlocharger Relationship

The engine combustion is dependent on the engine speed. As the engine speed increases the combustion exhaust temperature also increases causing the exhaust temperature to increase. The higher exhaust temperatures create a larger heat source for the Stirlocharger to capture as heat input. The higher heat input increases the Stirlocharger work output, which due to the coupling of the Stirlocharger with the compressor, increases the compressor speed. The increased speed of the compressor increases the engine intake boost pressure which increases engine combustion and therefore engine speed.

4.3 Pressure of Working Gas In Stirlocharger

The pressure within the Stirlocharger is defined by the ideal gas law:

$$PV = MRT \quad (\text{Eqn 1})$$

By manipulating eq (1) the pressure at a certain volume and temperature can be derived as,

$$P = \frac{MRT}{V_T} \quad (\text{Eqn 2})$$

To isolate $M * R$ in the numerator we divide both the numerator and denominator by T resulting in,

$$P = \frac{MRT}{V_T / T} \quad (\text{Eqn 3})$$

The total volume at any instant in the Stirlocharger is,

$$V_T = V_H + V_C + V_{RD} \quad (\text{Eqn 4})$$

The volume at any particular instant is a function of crank angle θ except the regenerator dead volume V_{RD} which is a constant, therefore defining the volume as a function of crank angle using eq (4),

$$V_T(\theta) = V_H(\theta) + V_C(\theta) + V_{RD} \quad (\text{Eqn 5})$$

Now inputting eq (5) into eq (3) we get,

$$P(\theta) = \frac{MR}{\frac{V_H(\theta)}{T_H} + \frac{V_C(\theta)}{T_C} + \frac{V_{RD}}{T_R}} \quad (\text{Eqn 6})$$

where,

P = Pressure of the working gas in the Stirlocharger (kPa)

M = Total mass of gas in the Stirlocharger (kg)

R = Ideal gas constant, $\left(287 \frac{J}{kg * K}\right)$

V_H = Volume of hot space (cm^3)

V_C = Volume of cold space (cm^3)

V_{RD} = Regenerator dead volume (cm^3)

T_H = Temperature of hot space (K)

T_C = Temperature of cold space (K)

T_R = Temperature within the regenerator (K)

4.4 β -Stirlocharger Power

The output power of the stirlocharger is equal to the power output of the stirling engine within it. The power of the stirling engine is defined by Cooke-Yarborough as,

$$\dot{W} = \frac{P_{mean}\omega}{8} \cdot \frac{V_E V_O}{V_M} \cdot \frac{\Delta T \sin(\alpha)}{T_C + \frac{V_C}{V_M} \Delta T} \quad (\text{Eqn 1})$$

where,

\dot{W} = Power output of the Stirlocharger (W)

P_{mean} = Mean pressure of the working gas, of pressure with both the displacer and power piston at mid stroke.

ω = Operating frequency. Using $2\pi \frac{rad}{sec}$ so that the output power in watts is

numerically equal to power per cycle (J)

$V_E = V_H$ = Volume of Hot Space (cm^3)

V_C = Volume of cold space (cm^3)

V_M = Total gas volume of the system when the output piston is at mid stroke (cm^3)

$$V_M = V_H + V_{RD} + \frac{V_C}{2}$$

ΔT = Difference between the hot and cold temperatures,

$$\Delta T = T_H - T_C$$

α = Phase angle of the Stirlocharger (90 deg)

4.5 α -Stirlocharger Power

The output power of the stirlocharger is equal to the power output of the stirling engine within it. The power of the stirling engine is defined by Walker & Schmidt as,

$$\dot{W} = p_{\max} V_T (\theta) \pi \cdot \frac{\tau - 1}{k + 1} \cdot \left(\frac{1 - \delta}{1 + \delta} \right)^{0.5} \cdot \frac{\delta(\sin(\theta))}{1 + (1 + \delta^2)^{0.5}} \quad (\text{Eqn 1})$$

Where,

P_{\max} = Maximum pressure of the working gas (MPa)

V_T = Total volume of hot and cold space (cm³)

τ = Ratio of hot and cold temperature

$$\delta := \frac{\left(\tau^2 + 2 \cdot \tau \cdot k \cdot \cos(90) + k^2 \right)^{0.5}}{\tau + k + 2 \cdot S}$$

4.6 Compressor Speed of Stirlocharger

The relationship between Power, Torque and Speed is defined by,

$$P(kW) = \frac{N(rpm)T(Nm)}{9549} \quad (\text{Eqn 1})$$

The Speed can be derived using eq (1) and put in the form,

$$N(rpm) = \frac{P(kW) * 9549}{T(Nm)} \quad (\text{Eqn 2})$$

The power has been defined in eq (1) from section 4.2 and can be inserted into equation (2) above to get,

$$N(\text{rpm}) = \frac{\left[\frac{P_{\text{mean}} \omega}{8} \cdot \frac{V_E V_O}{V_M} \cdot \frac{\Delta T \sin(\alpha)}{T_C + \frac{V_C}{V_M} \Delta T} \right] * 9549}{T(\text{Nm})} \quad (\text{Eqn 3})$$

where,

N = Speed of the Stirlocharger compressor impeller (RPM)

T = Static Torque of the Stirlocharger compressor impeller (Nm)

4.7 Compressor Boost Pressure

The boost pressure of the Stirlocharger compressor is dependent on the impeller and compressor outlet geometry. The peripheral velocity of the compressor impeller is defined by,

$$V_{\text{peripheral}} = N * D_{\text{impeler}} \quad (\text{Eqn 1})$$

The compressor head can then be calculated using eq (1),

$$H = \frac{(V_{\text{peripheral}})^2}{2 * g} \quad (\text{Eqn 2})$$

The pump outlet pressure can then be calculated using eq (2),

$$P_{\text{pump}} = 0.433 * H * SG_{\text{air}} \quad (\text{Eqn 3})$$

The impellor flow compensation is defined by,

$$V_{\text{flowcomp}} = 5E - 5 * N \quad (\text{Eqn 4})$$

The pressure ration between the inlet and outlet of the compressor is then calculated by,

$$\pi_C = (0.9244 * V_{\text{flowcomp}}) + 1.0331 \quad (\text{Eqn 5})$$

The compressor boost pressure can then be calculated using eq (5),

$$P_{Boost} = (\pi_c * P_{in}) - P_{in} \quad (\text{Eqn 6})$$

where,

P_{Boost} = Boost pressure of the compressor (*kPa*)

π_c = Compressor pressure ratio

P_{in} = Compressor Inlet pressure (*kPa*)

4.8 Stirlocharger Compressor Mass Flow Rate

The compressor power is defined as:

$$P_C = \frac{\dot{m}_c \Delta h_{s,C}}{\eta_c \eta_{m,C}} \quad (\text{Eqn 1})$$

where,

P_C = Compressor pressure (*kPa*)

\dot{m}_c = Compressor air mass flow rate (*kg / s*)

$\Delta h_{s,C}$ = Compressor isentropic enthalpy increase

η_c = Isentropic compressor efficiency

$\eta_{m,C}$ = Mechanical compressor efficiency

The Stirling engine power output is defined in section 4.2, and is re-written here:

$$\dot{W} = \frac{P_{mean} \omega}{8} \bullet \frac{V_E V_O}{V_M} \bullet \frac{\Delta T \sin(\alpha)}{T_C + \frac{V_C}{V_M} \Delta T} \quad (\text{Eqn 2})$$

The Compressor is powered by the Stirling engine, therefore equating (1) and (2):

$$\dot{W} = \frac{\dot{m}_C \Delta h_{s,C}}{\eta_C \eta_{m,C}} \quad (\text{Eqn 3})$$

Isolating the compressor mass flow rate \dot{m}_C in eq (3):

$$\dot{m}_C = \frac{\dot{W}(\eta_C \eta_{m,C})}{\Delta h_{s,C}} \quad (\text{Eqn 4})$$

The compressor isentropic enthalpy increase is defined as:

$$\Delta h_{s,C} = R_A T_1 \frac{k_A}{k_A - 1} \left[\left(\frac{p_2}{p_1} \right)^{\frac{k_A - 1}{k_A}} - 1 \right] \quad (\text{Eqn 5})$$

Inserting (5) into (4):

$$\dot{m}_C = \frac{\dot{W}(\eta_C \eta_{m,C})}{R_A T_1 \frac{k_A}{k_A - 1} \left[\left(\frac{p_2}{p_1} \right)^{\frac{k_A - 1}{k_A}} - 1 \right]} \quad (\text{Eqn 6})$$

where,

$$R_A = \text{Ideal gas constant of air, } \left(287 \frac{J}{kg * K} \right)$$

T_1 = Compressor inlet air temperature (K)

p_1 & p_2 = Pressures at compressor inlet and outlet respectively (kPa)

$$k_A = \frac{c_p}{c_v} = 1.4$$

4.9 Stirlocharger Thermal Efficiency

The general definition of efficiency is the ratio of the work out to the energy in shown

by,

$$(\eta_m)_{Stirlochager} = \frac{W_{out}}{Q_{in}} \quad (\text{Eqn 1})$$

4.10 Response Time of Stirlochager

The response time τ_{90} of a turbocharger is (Schafer, 2012):

$$\tau_{90} \approx \frac{\Omega_{90}^2 I_p}{\eta_m P_T} \quad (\text{Eqn 1})$$

In the Stirlochager the power of the turbine P_T is replaced by the power output of the Stirling engine \dot{W} . Inserting stirling engine power out in (1):

$$\tau_{90} \approx \frac{\Omega_{90}^2 I_p}{(\eta_m)_{Stirlochager} \dot{W}} \quad (\text{Eqn 2})$$

where,

τ_{90} = Time required to reach 90% of maximum engine torque

Ω_{90} = Rotor speed at 90% of maximum engine torque

I_p = Polar mass inertia moment of the rotor $I_p = \frac{m^* r^2}{2} \left(\frac{kg^* in^2}{2} \right)$

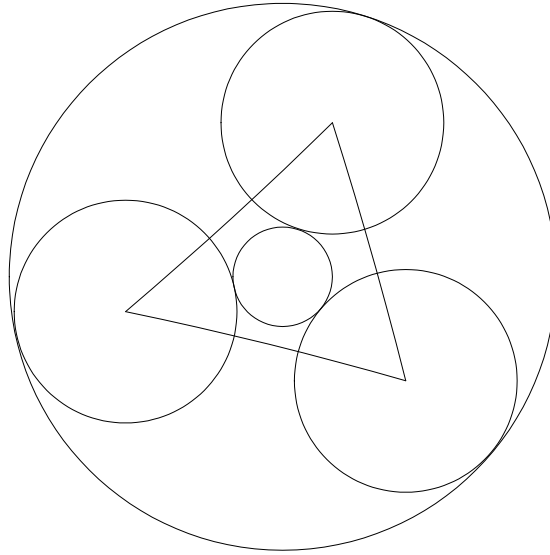
4.11 Gear Train Analysis

Figure 4-1: Planetary Gear Train Schematic

For a ring gear with teeth N_r of 100, and a sun gear N_s with teeth 10, the required teeth for the planet gear N_p is given by:

$$N_p = \frac{N_r - N_s}{2} = \frac{100 - 10}{2} = 45$$

The carrier angular momentum ω_c is found by converting the carrier RPM:

$$\omega_c = 1000 \frac{\text{rev}}{\text{min}} \left(\frac{2\pi \text{rad}}{1 \text{rev}} \right) \left(\frac{1 \text{min}}{60 \text{sec}} \right) = 104.667 \frac{\text{rad}}{\text{sec}}$$

The angular momentum of the planet gear ω_p is:

$$\omega_p = \frac{-(N_r - N_p)\omega_c}{N_p} = \frac{-(100 - 45) \left(104.667 \frac{\text{rad}}{\text{sec}} \right)}{45} = -127.926 \frac{\text{rad}}{\text{sec}}$$

The angular momentum of the sun gear ω_s is then:

$$\omega_s = \frac{(N_s + N_p)\omega_c - N_p\omega_p}{N_s} = \frac{(10 + 45)104 \frac{rad}{sec} - \left[45 \left(-127.926 \frac{rad}{sec} \right) \right]}{10} = 1151.335 \frac{rad}{sec}$$

The final sun gear speed in RPM is then:

$$(RPM)_s = 1151.335 \frac{rad}{sec} \left(\frac{1 rev}{2\pi rad} \right) \left(\frac{60 sec}{1 min} \right) = 11000.016 rpm$$

4.12 Numerical Simulations

4.12.1 β -Stirlocharger

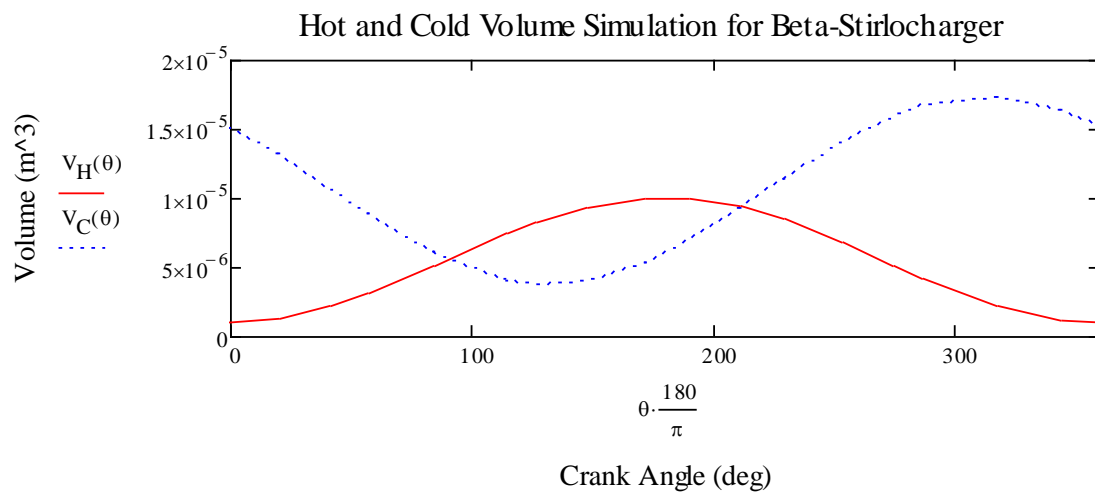


Figure 4-2: The variation in the hot and cold volumes of the β -Stirlocharger.

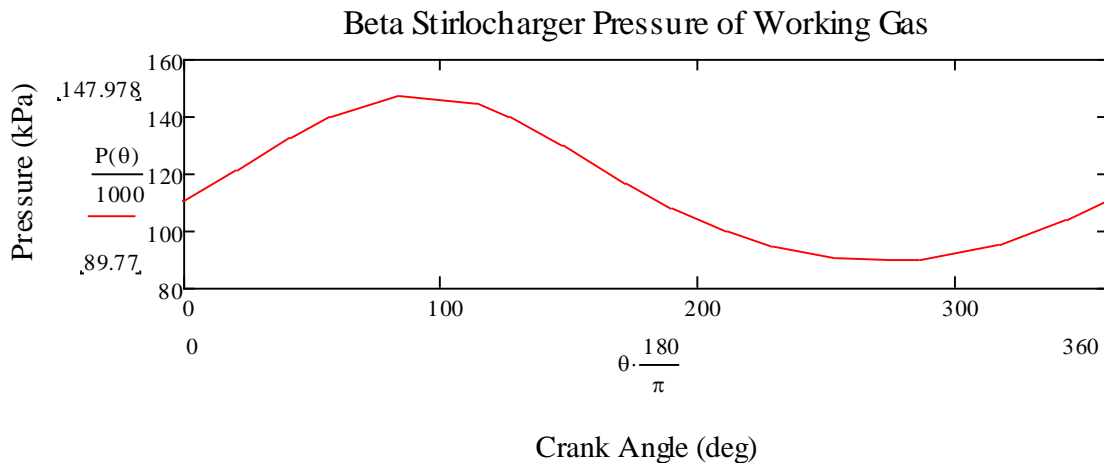


Figure 4-3: The pressure of the β -Stirlocharger is shown with respect to the crank angle. The peak pressure is 147.98 kPa.

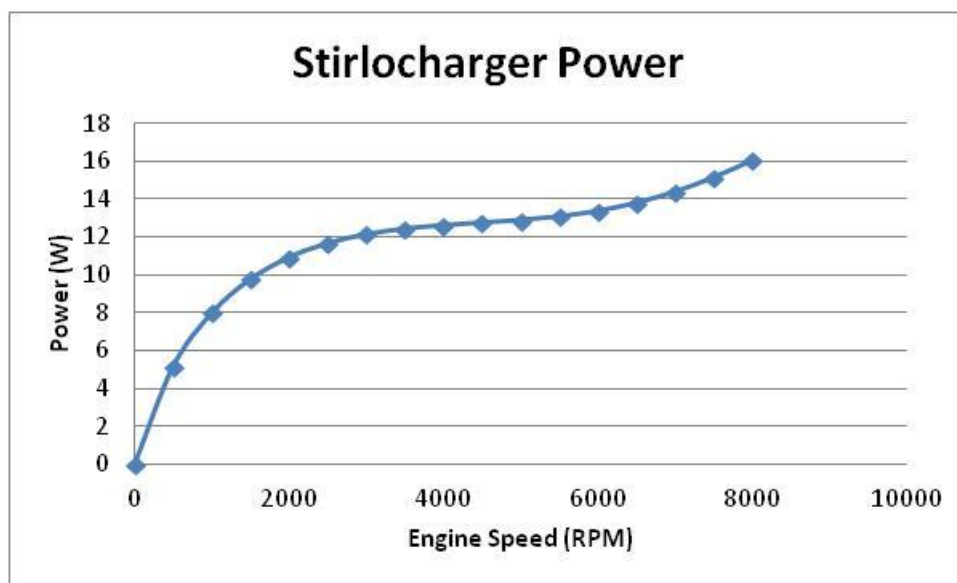


Figure 4-4: The simulated power of the β -Stirlocharger using the equations described in section 4.2.

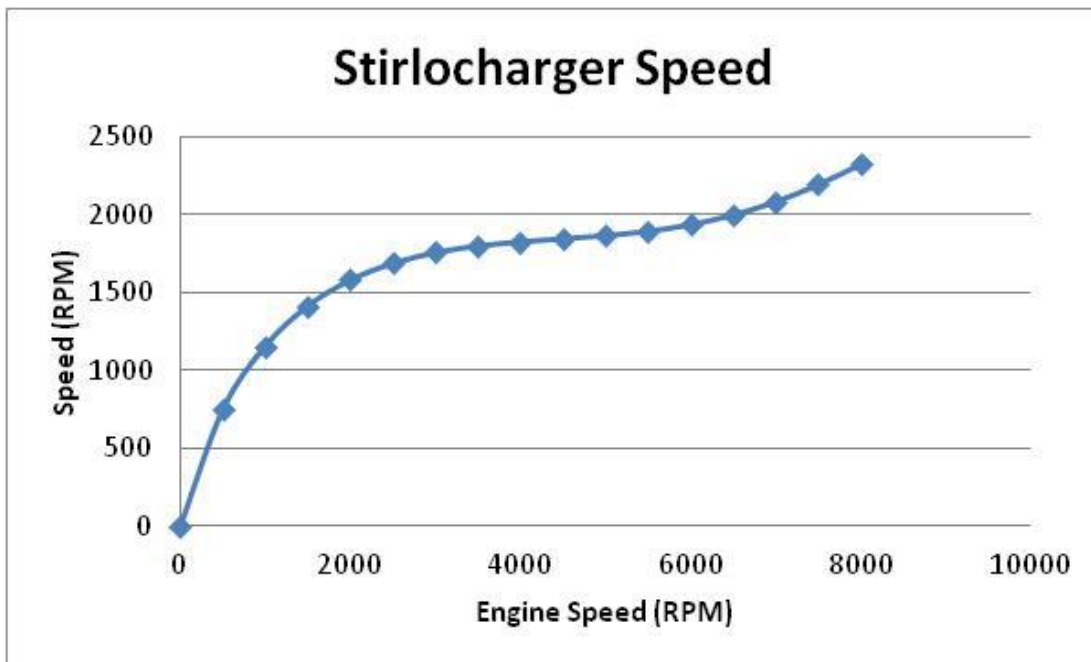


Figure 4-5: Simulated Speed of the β -Stirlocharger using the equations in described in section 4.3.

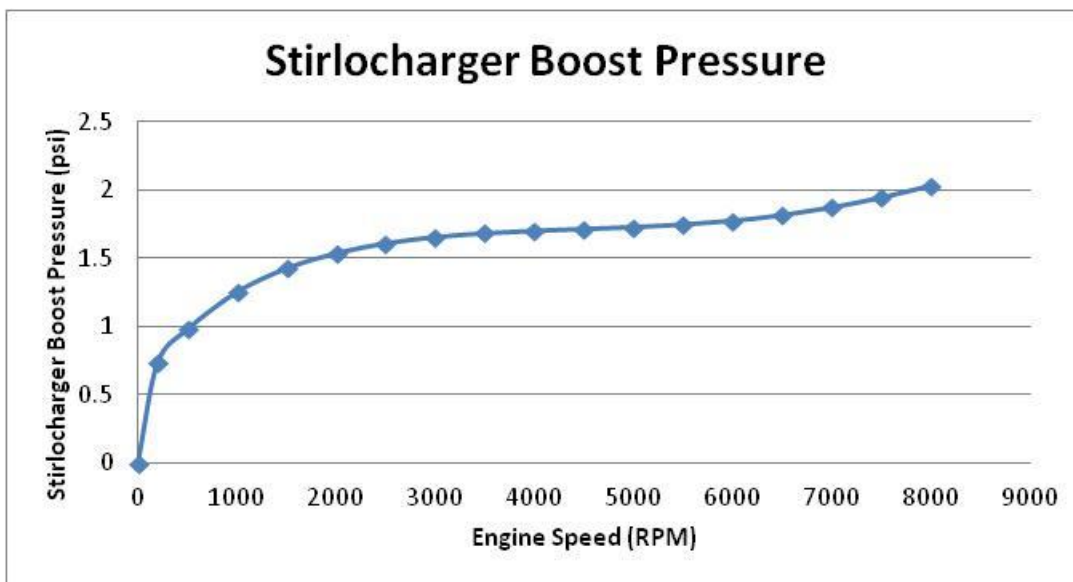


Figure 4-6: Simulated output Boost Pressure of the β -Stirlocharger.

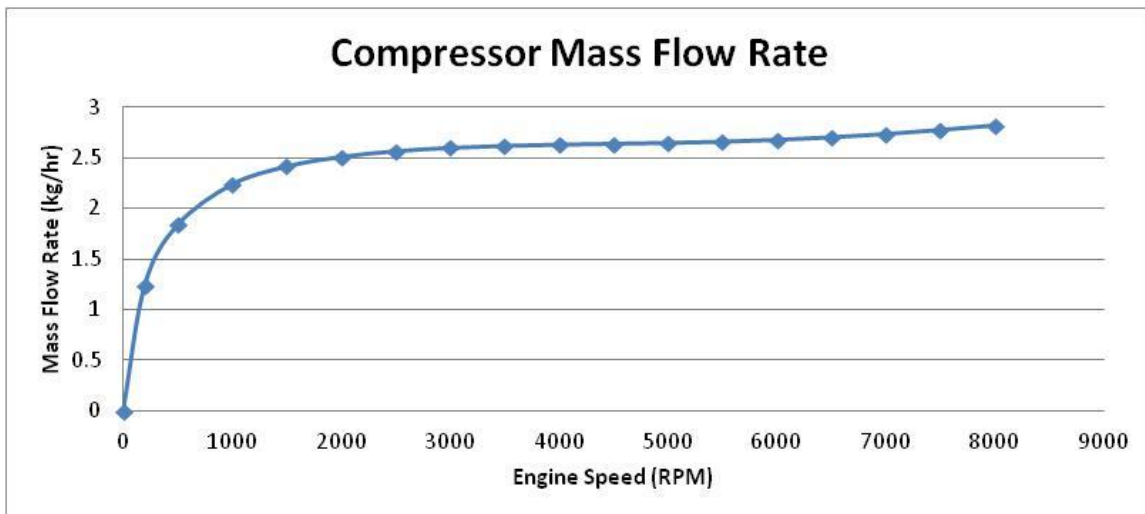


Figure 4-7: Simulated mass flow rate of air through the β -Stirlocharger compressor.

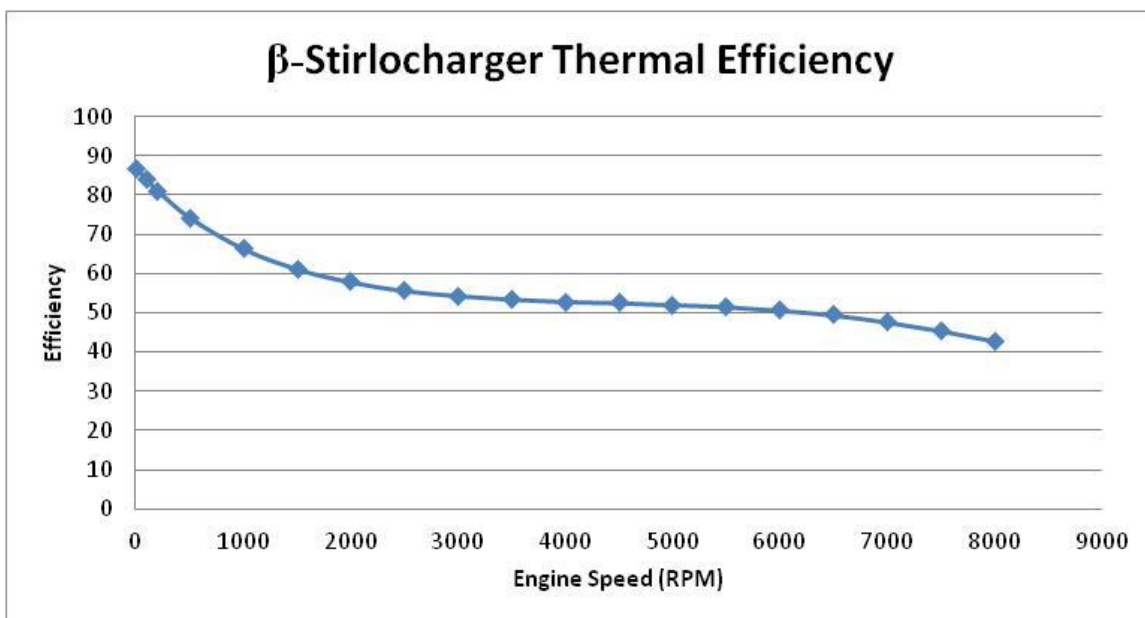


Figure 4-8: Simulated β -Stirlocharger thermal efficiency.

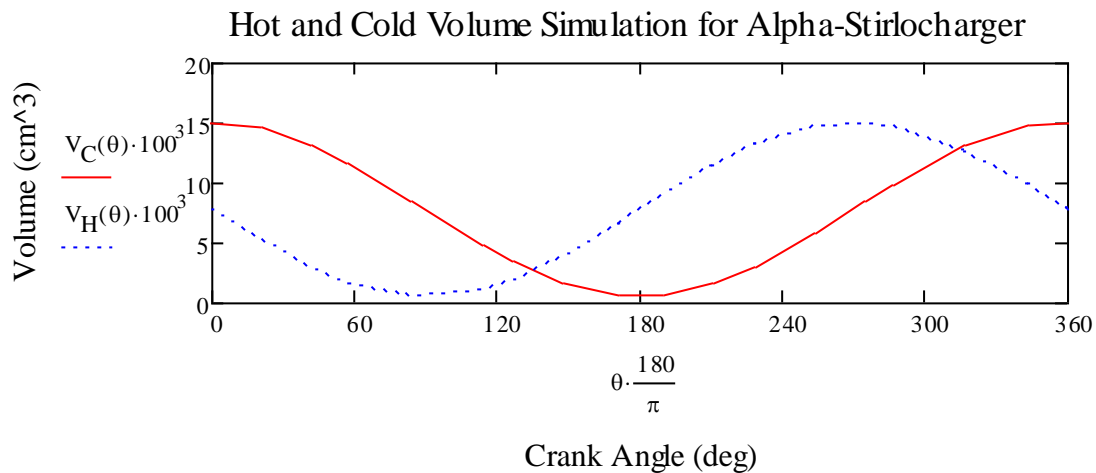
4.12.2 α -Stirlocharger

Figure 4-9: The variation in the hot and cold volumes of the α -Stirlocharger.

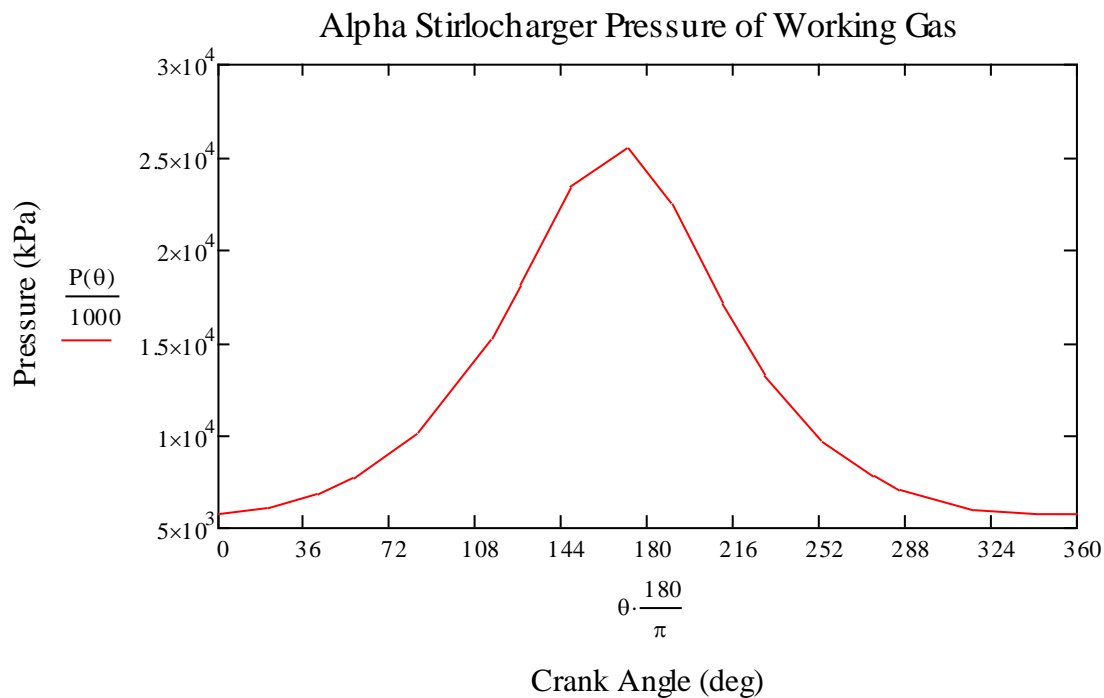


Figure 4-10: The pressure of the α -Stirlocharger is shown with respect to the crank angle. The peak pressure is 2550 kPa.

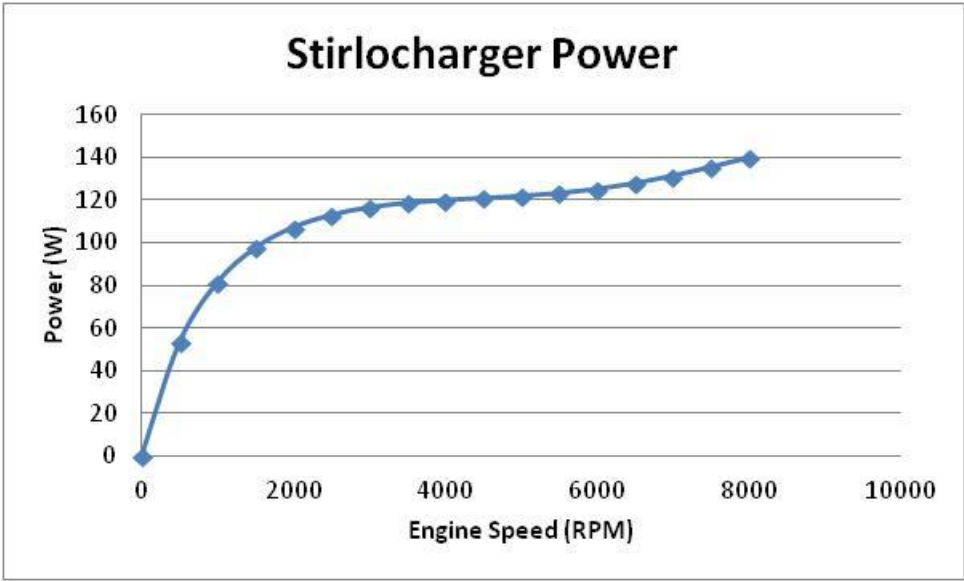


Figure 4-11: The simulated power of the α -Stirlocharger using the equations described in section 4.2.

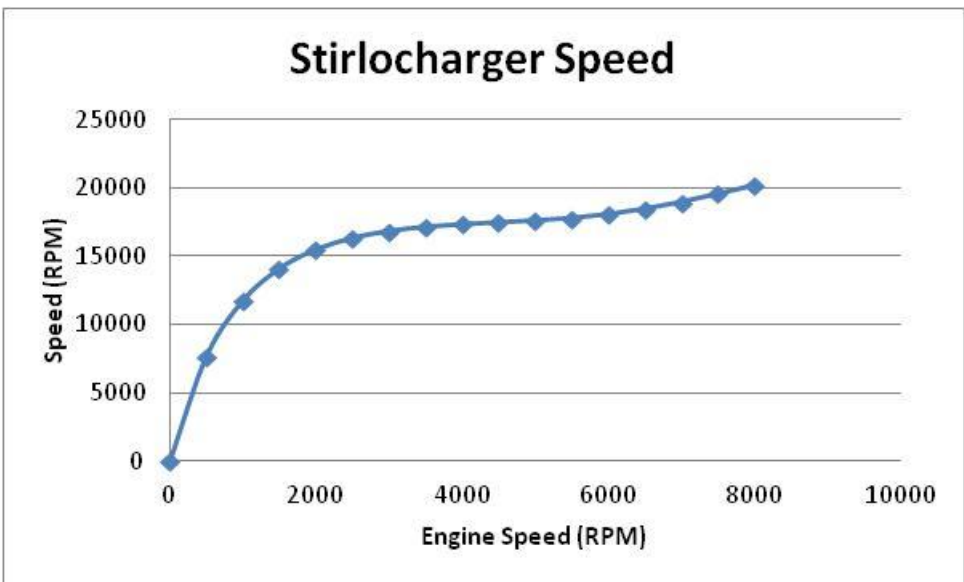


Figure 4-12: Simulated Speed of the α -Stirlocharger using the equations in described in section 4.3.

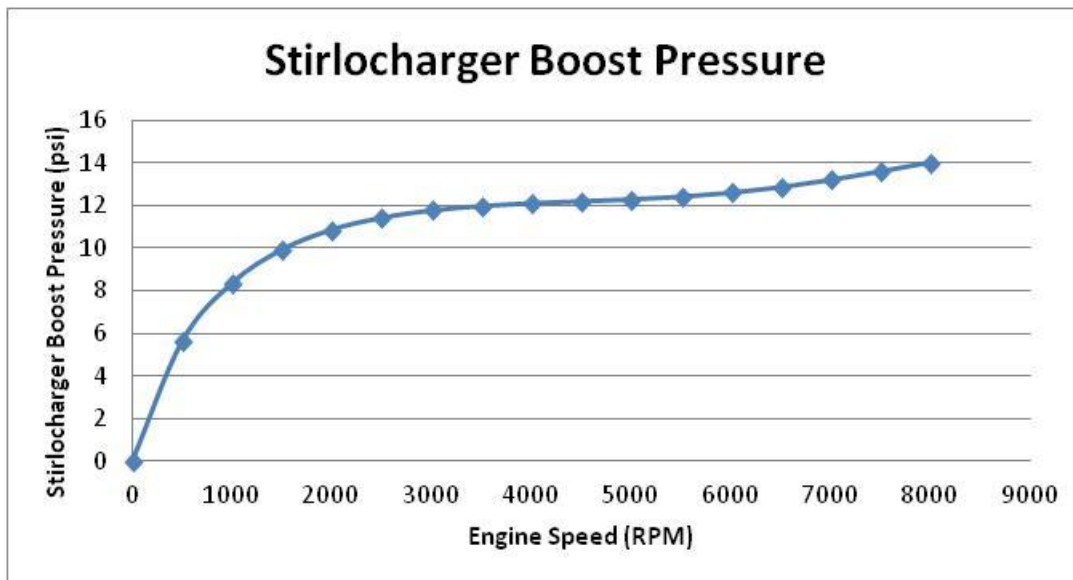


Figure 4-13: Simulated output Boost Pressure of the α -Stirlocharger.

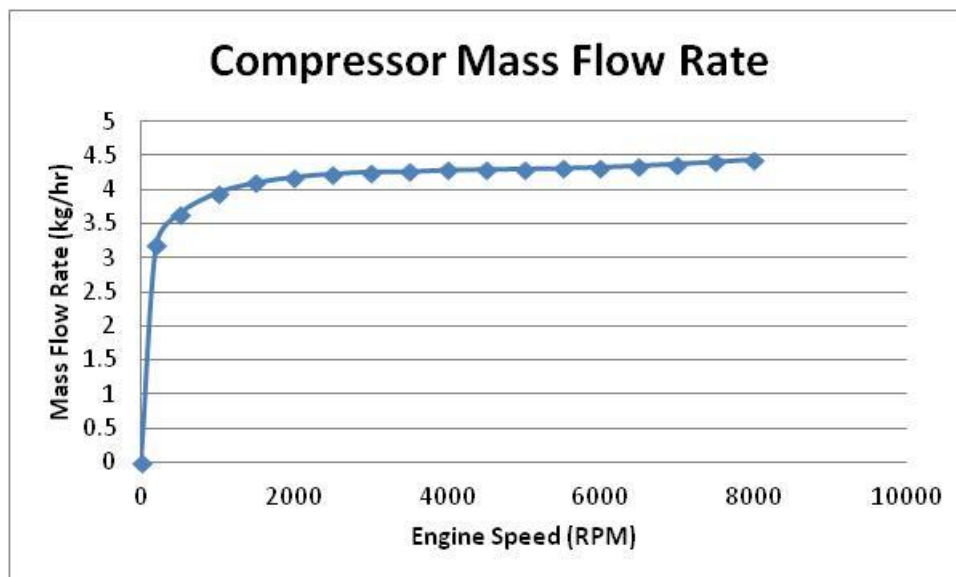


Figure 4-14: Simulated mass flow rate of air through the α -Stirlocharger compressor.

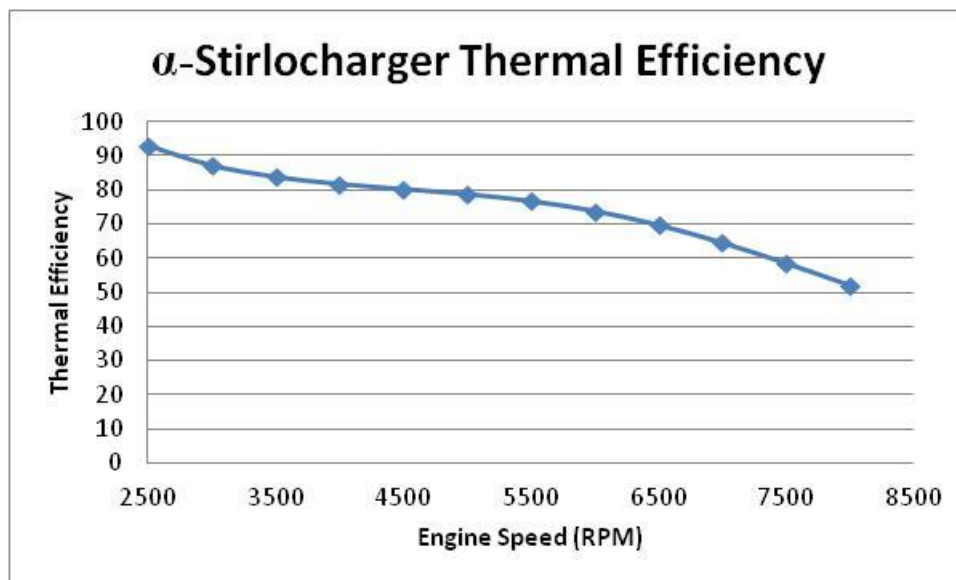


Figure 4-15: Simulated β -Stirlocharger thermal efficiency.

CHAPTER 5 SUMMARY, CONCLUSIONS AND RECOMMENDATIONS

5.1 MODEL

Computer 3D models were first created of two Stirlocharger concepts namely the β -Stirlocharger and the α -Stirlocharger using Solid Works. These concepts are accurate, manufacturable and installable on the lab test diesel engine Yanmar 4TNV84T-ZDSAD.

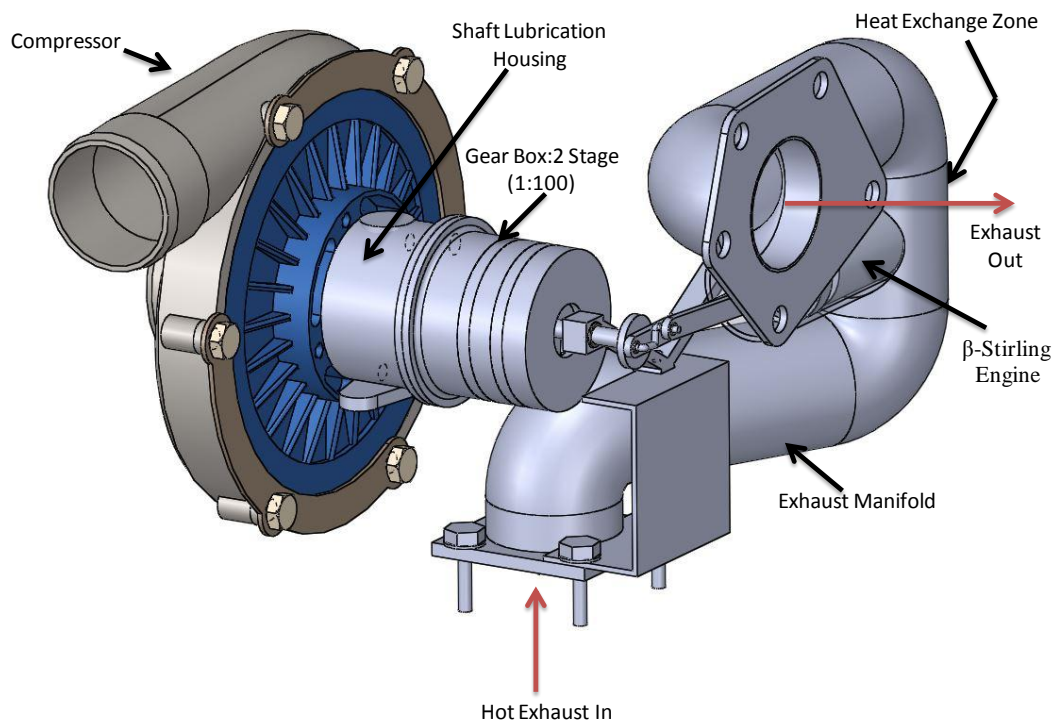
5.1.1 3D Model of the β -Stirlocharger

Figure 5-1: β -Stirlocharger 3D Model Schematic

The beta design was the initial conception of the Stirlocharger. The β -Stirling engine was used in this design due to its reduced complexity in design and ease of implementation. It is a single axis design which consumes less installation space, and also has a high power to size ratio. The engine specifications are shown in table 5-1. The complete schematic of the device is detailed in Appendix 6.1.

Table 5-1: β -Stirlocharger Specifications

β-Stirlocharger Specifications	
Bore (in)	1.61
Stroke (in)	1
Cylinder Material	Copper
Piston Material	Aluminium
Crank Radius (in)	0.75
Gear Ratio	1:100

5.1.2 3D Model of the α -Stirlocharger

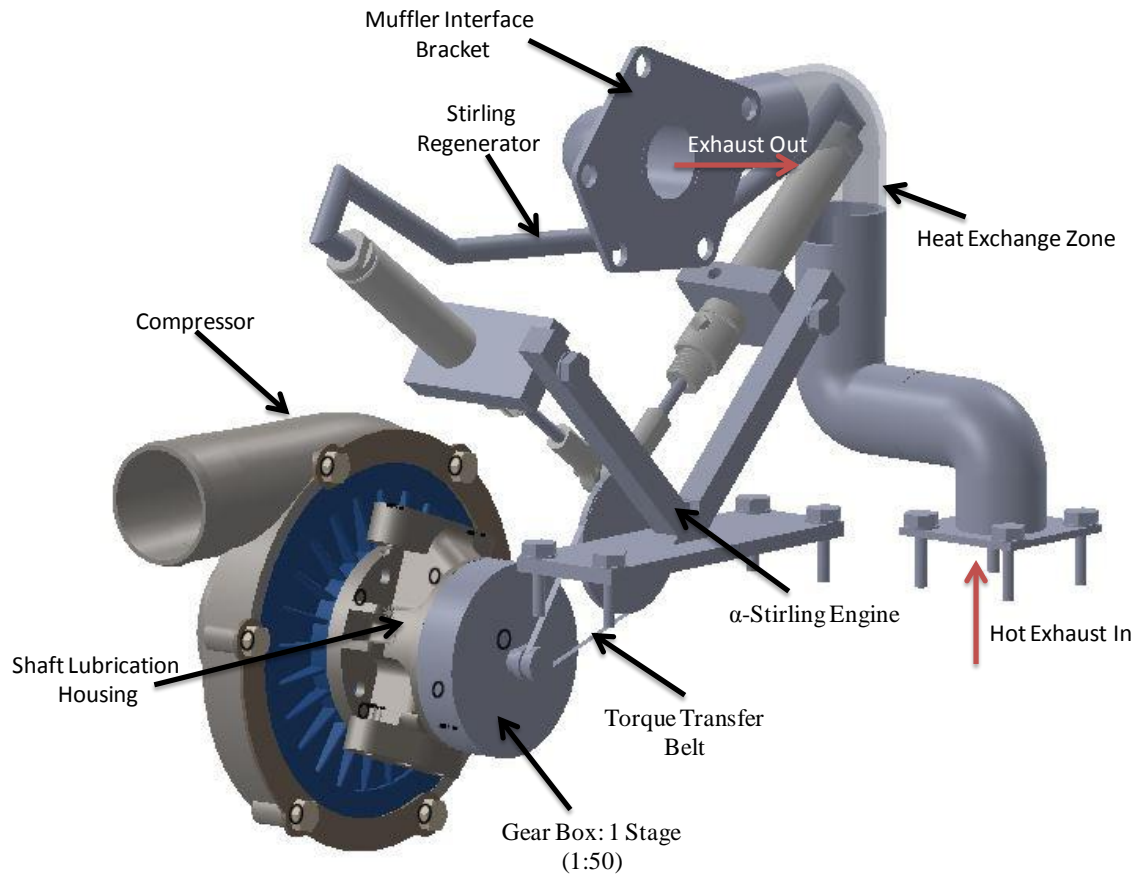


Figure 5-2: α -Stirlocharger 3D Model Schematic

The α -Stirlocharger was a second design primarily focused at a higher power to size ratio design using an α -Stirling engine. This design is a V-shaped, dual axis and uses two single seal stainless steel cylinders. The speed of this design is greater than the β -Stirlocharger due to the smaller bore size of 3/4". The specifications are shown in table 5-2. The axis of the cylinders is variable and not fixed with respect to one another. As the main cylinder rotates, the cylinders pivot to minimize friction by keep the linear piston thrust force normal to the translational axis of the cylinder. This principle is pictured below:

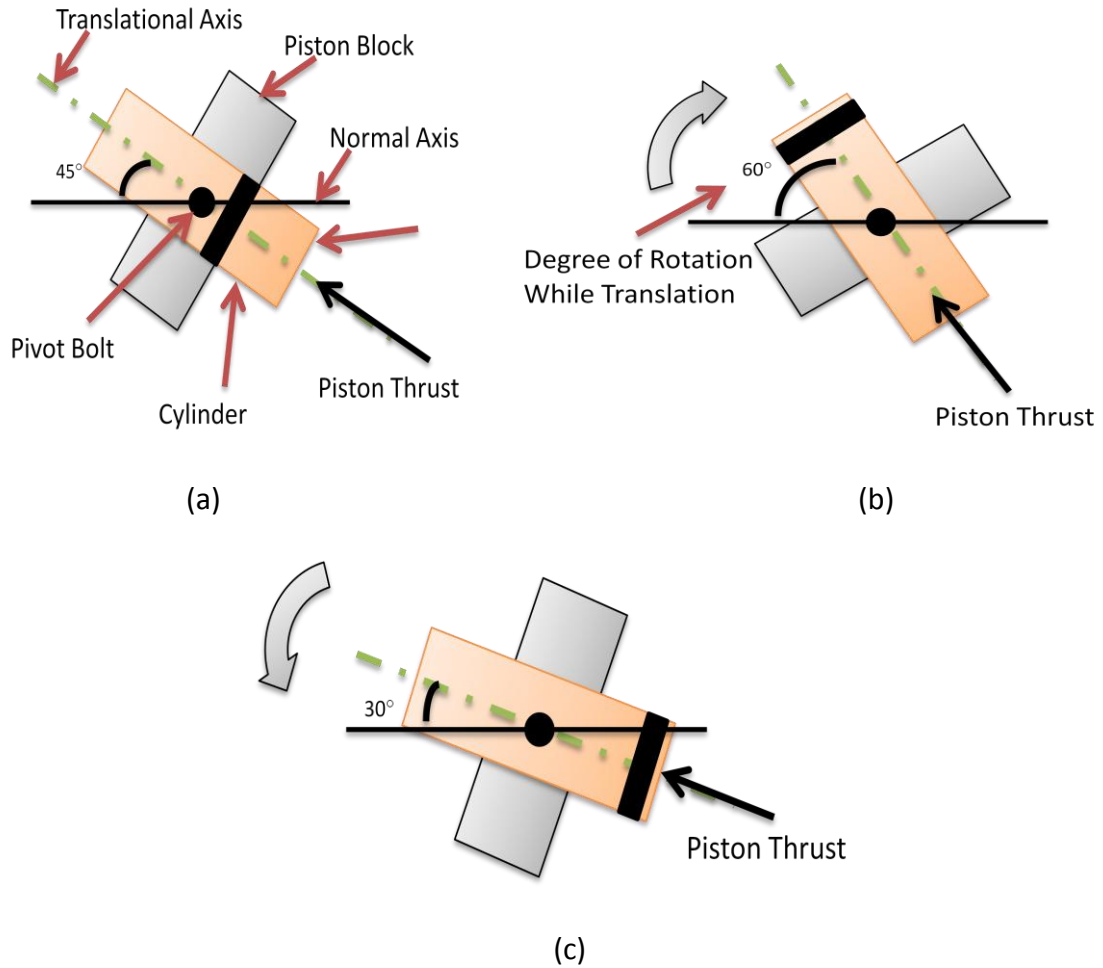


Figure 5-3: α -Stirlocharger Piston-Cylinder Rotational Schematic. (a) Normal position of the piston-cylinder, piston near pivot. (b) Piston-Cylinder rotates 15° CW as Piston approached TDC. (c) Piston-Cylinder rotates 15° CCW as Piston approached BDC.

Table 5-2: α -Stirlocharger Specifications

α-Stirlocharger Specifications	
Bore (in)	0.75
Stroke (in)	2.5
Cylinder Material	Stainless Steel
Piston Material	Aluminum
Crank Radius (in)	2
Gear Ratio	1:50

5.2 MANUFACTURED PROTOTYPE

The 3D models were detailed and manufactured to build real world prototypes for the purposes of testing and data acquisition. The parts were manufactured at the Purdue Artisan and Fabrication Laboratory (AFL).

5.2.1 β -Stirlocharger Prototype



Figure 5-4: β -Stirlocharger

This prototype was designed, manufactured and tested. Due to the low accuracy of manufacturing and relatively loose tolerance levels, the prototype did not perform as anticipated. The friction between the piston and cylinder wall was high, this was caused by the piston edge hitting the cylinder wall due to a bending moment caused by the connecting rod and the larger clearance distance between the two components. This bending issue is explained schematically in Figure 5-5 and Figure 5-6.

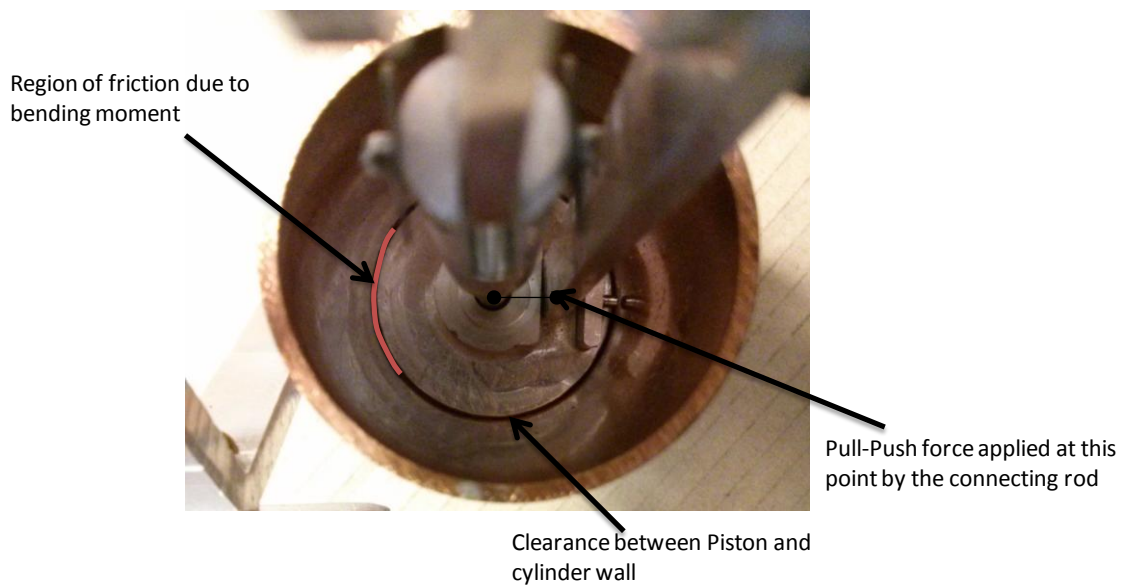


Figure 5-5: Interior cylinder friction Zone

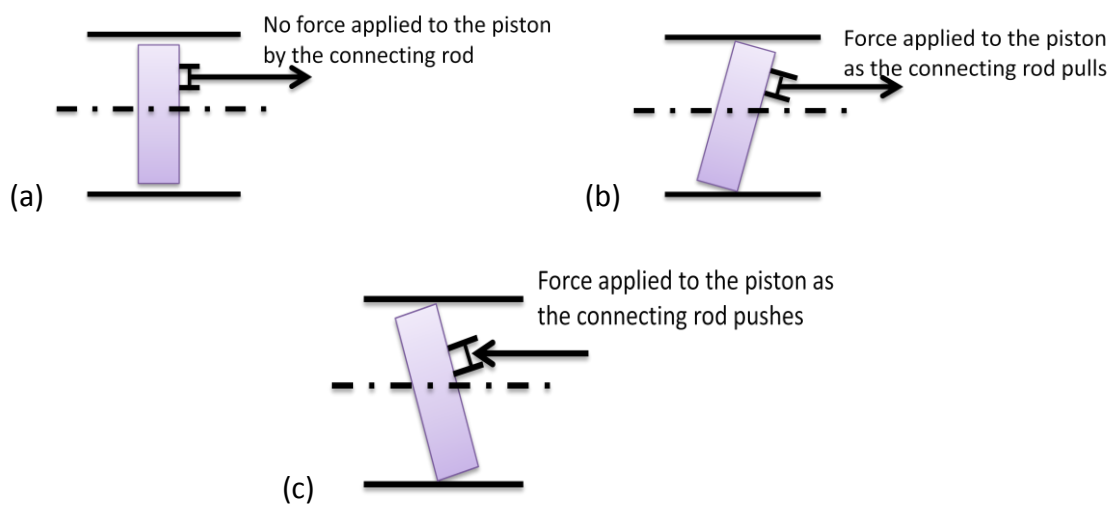


Figure 5-6: Force acting on the piston for (a) Stationary condition, (b) Pulling outward condition, (c) Pushing inward condition

5.2.2 α -Stirlocharger Prototype



Figure 5-7: α -Stirlocharger

This prototype was designed and manufactured after the β -Stirlocharger. This prototype didn't perform as expected due to the low accuracy of manufacturing. In this double axis design, two pneumatic air-cylinders were used, one exposed to the hot exhaust side and the other to the cold side. The primary reason of failure of this model was the error in precision manufacturing of the pivot shaft shown in Figure 5-8.

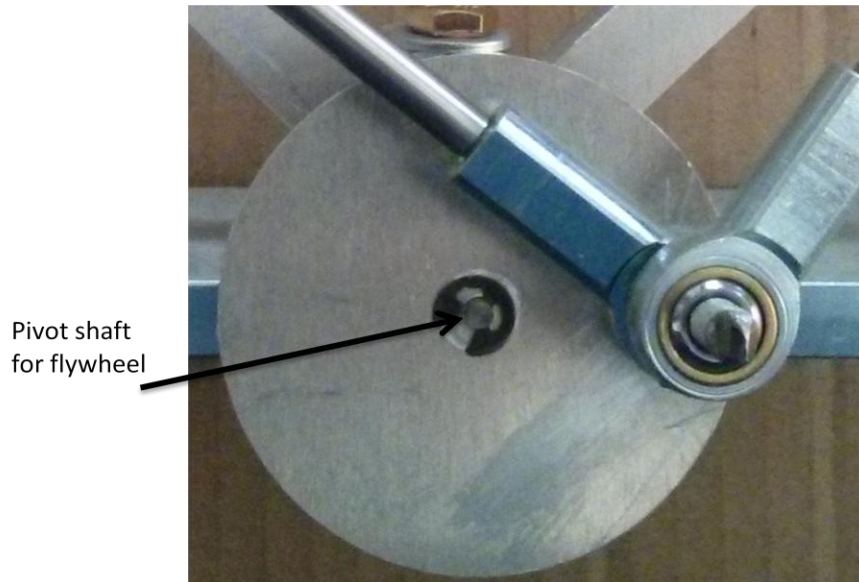


Figure 5-8: α -Stirlocharger Flywheel Pivot

5.3 Baseline Tests

5.3.1 Torque Test on Compressor Impellor

A torque test was conducted to measure the minimum torque required to rotate the compressor impellor. The test engine is equipped with an IHI turbocharging system. The compressor was installed on a test stand keeping the impellor shaft horizontal with the table. An internally manufactured arm was attached to the impellor hub hole with an arbitrary length. A measured weight W was attached to the end of the arm using a thin thread. The distance of the thread was varied from the hub center and the distance r was measured as soon as the impellor overcame its static friction. The torque was calculated using the fundamental equation for torque Eqn 5.1. Three experimental calculations were performed based on the distance r at which the impeller showed signs

of initial rotation by overcoming its static friction, and the average torque was used as a bases for further analysis. Refer to Appendix A for calculation method.

$$T = r * W \quad (\text{Eqn: 5.1})$$

Where,

r = Arm length,

W = Weight of load

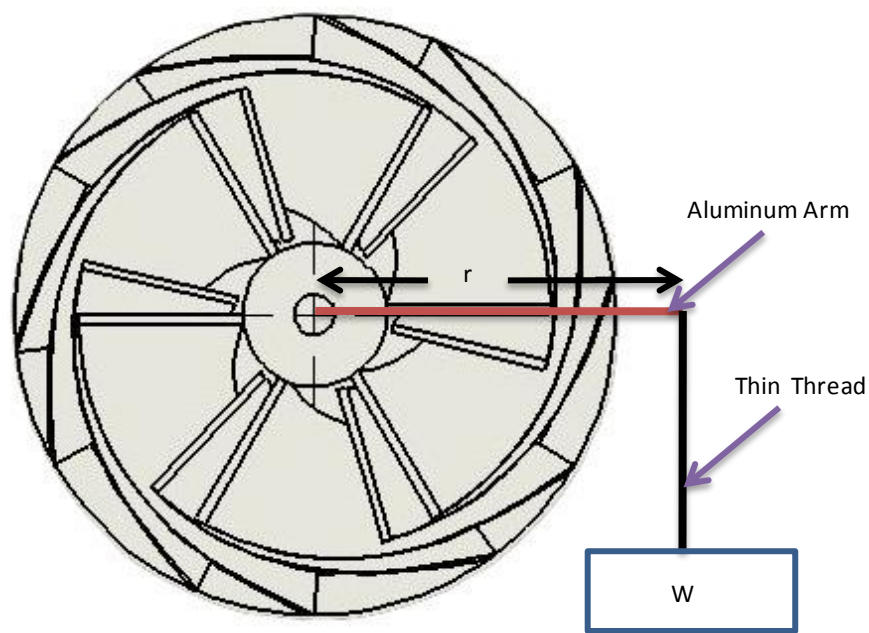


Figure 5-9: Impellor with Aluminum arm and thread loading

5.4 Turbine Backpressure Measurement Test

The backpressure of the turbocharger is critical and needs to be quantified by testing. The backpressure is generated due to the load induced by the compressor onto

the turbine. This reverse load slows down the turbine impellor speed and causes pressure build up in the exhaust manifold of the engine.

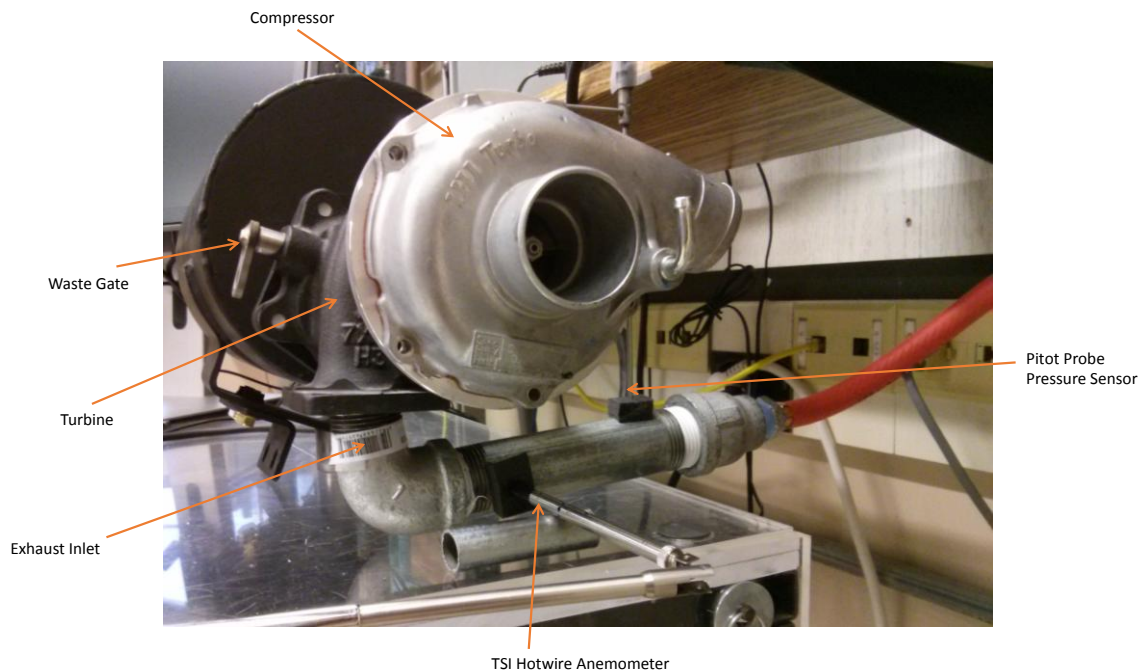


Figure 5-10: Backpressure Test Bench

The turbine test apparatus is shown in figure 5-5. The in-cylinder pressure and temperature at TDC for the engine at the onset of the exhaust stroke is 104.447psi and 1950.362 K. Ideally an air pressure of 104.447psi should be used for the test, but the laboratory is provided with a maximum air pressure rating of 80psi, thus 80psi is used for this test. The differential pressure and air velocity measurements are taken at the inlet manifold of the turbine without and with the compressor connected to the turbine as shown in Figure 5-3 and Figure 5-4 respectively. For this testing the waste gate was

fully closed, and all the air passed through the impellor. The dynamic pressure ζ in the exhaust manifold can be calculated using air velocity v_{air} by:

$$\zeta = \frac{1}{2} \rho_{air} (v_{air})^2$$

where,

ζ = Back pressure (Pa)

ρ_{air} = Air density at exhaust temperature (kg/m^3)

v_{air} = Air velocity (m/sec)

5.4.1 Turbine without the compressor attached

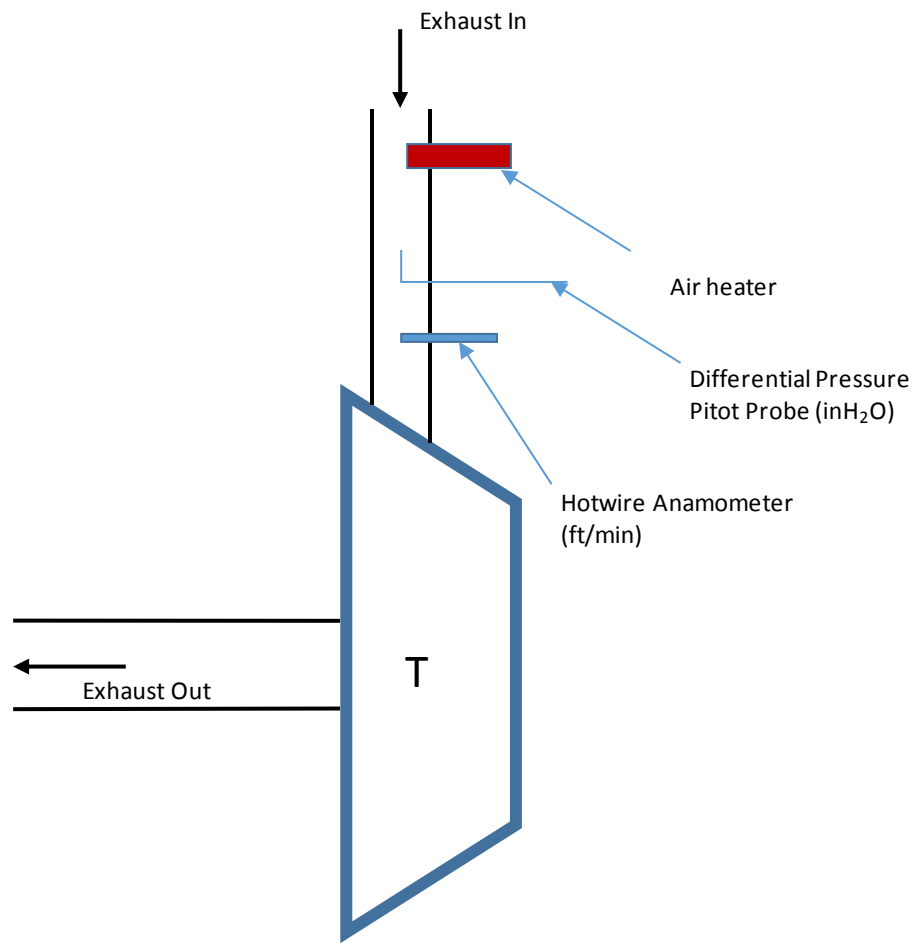


Figure 5-11: Backpressure test schematic without compressor

The measurements are taken once the system is at steady state and the turbine rotor is spooled up to speed. It is expected that once the compressor is attached to the turbine, the air velocity will reduce due to impeller induced inertia, and the differential pressure will rise showing a back pressure present.

5.4.2 Turbine with the compressor attached

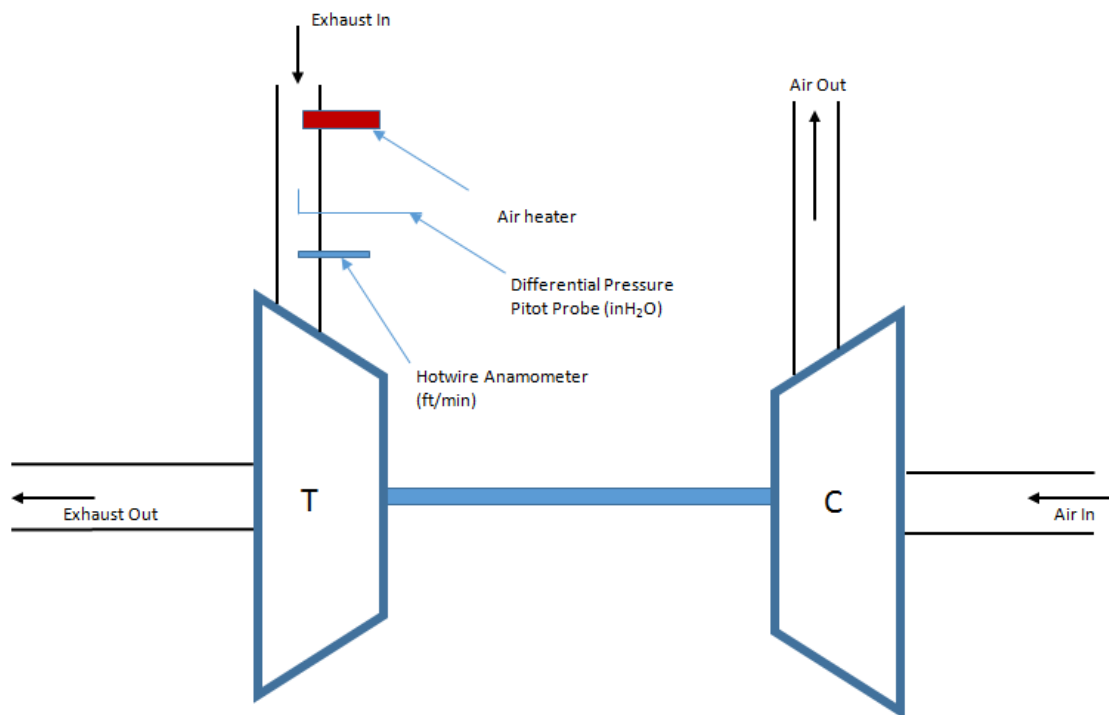


Figure 5.3: Backpressure test schematic with compressor

5.4.3 Backpressure Test Results

The backpressure test bench is shown in Fig 5-2 is used for testing the turbocharger assembly. The two configurations were tested, the air velocity and pressure in the

exhaust manifold was measured. The backpressure can be observed by inspecting Figure 5-4 and Figure 5-5. Once the compressor was added to the system assembly, the air velocity dropped by an average of 248.91 ft/min and the static pressure increased by an average of 0.061 inH₂O.

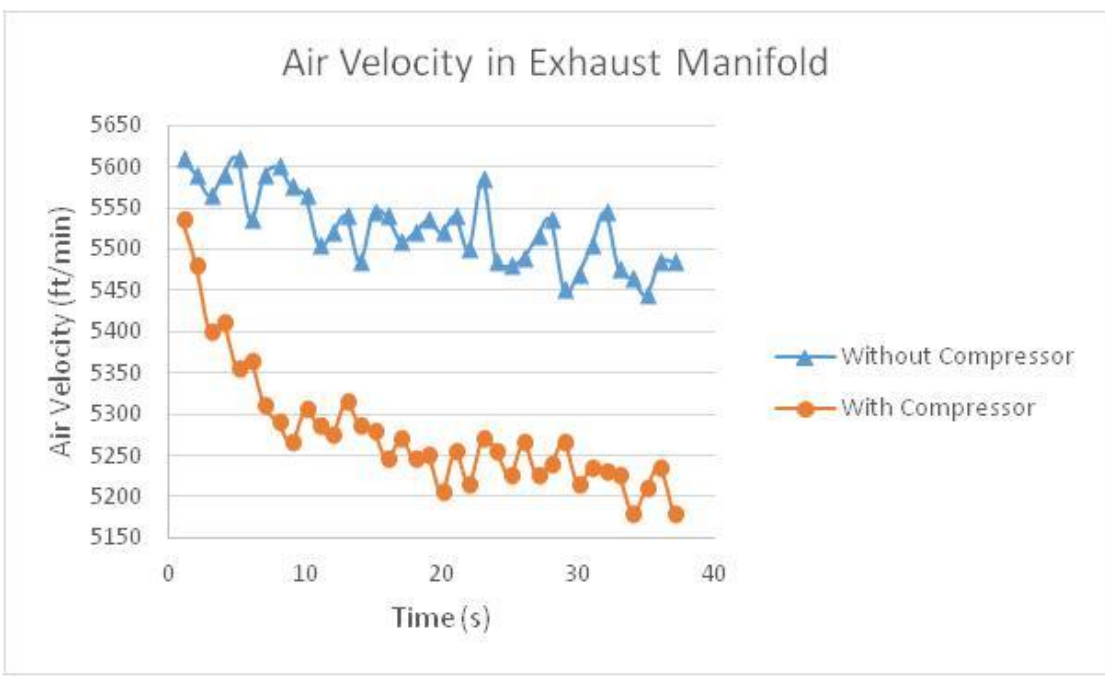


Figure 5-12: Air velocity measurements taken within the exhaust manifold of the test bench

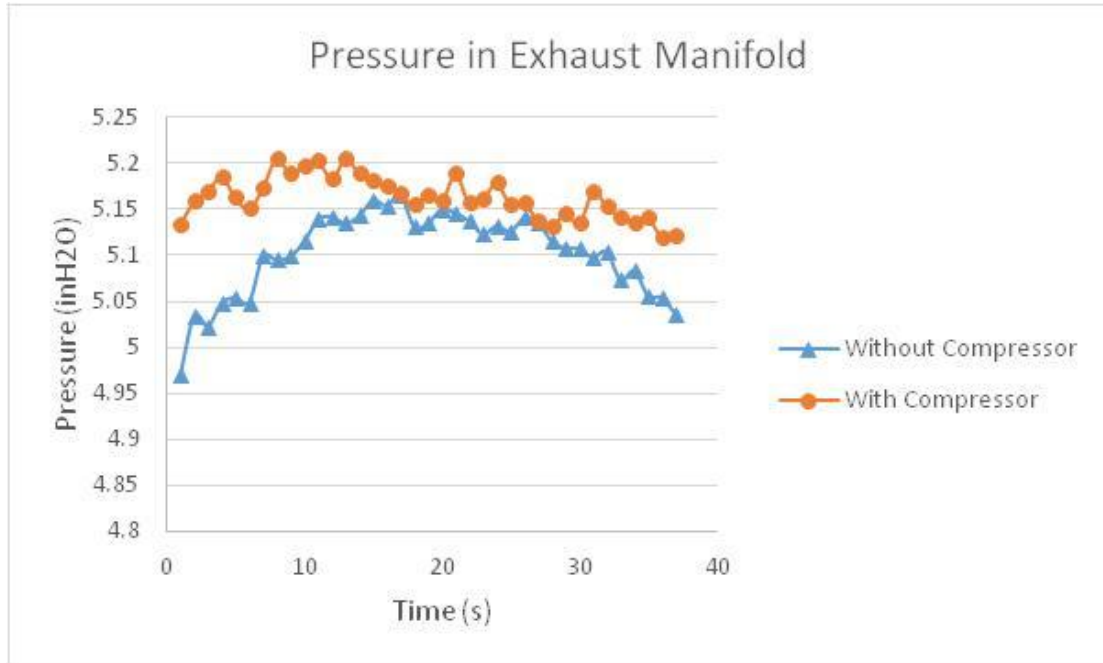


Figure 5-13: Pressure Differential measurements taken within the exhaust manifold of the test bench

5.5 Conclusions

The Stirlocharger is a feasible concept for waste energy recovery in automotive applications. Due to its nature of using heat as an energy source it's application is also feasible in other areas such as aerospace, and marine.

5.5.1 Design

In this thesis two theoretical Stirlocharger prototypes were designed numerically using two different stirling engine designs, an α -engine and a β -engine. The α -Stirlocharger consists of an α -Stirling engine and the β -Stirlocharger consists of the β -stirling engine. These Stirlocharger concepts are modeled using 3D modeling software keeping in consideration their integration with the engine and the exhaust manifold.

The models for both the designs as well as their specifications are shown in section 5.1. The α -Stirlocharger is considerable larger in both bore and stroke as compared to the β -Stirlocharger. This increase in engine size was chosen to compare the performance of a larger size engine with the smaller β -engine. The α -Storlocharger piston-cylinder assembly is an off the shelf hardware part bought from McMaster.

There is a significant design difference between the β and α stirlochargers, the β -Stirlocharger has an inherently compact design as the power piston and displacer reciprocate within one cylinder. This compact nature is ideal of on road automotive applications as space is of a significant constraint. However, with a smaller size the power is also reduced which will be discussed in the performance section of this thesis. The torque of any reciprocating engine is defined by

$$T = F * r$$

where,

F = Force

r = radius or offset distance from the central axis

Considering the torque equation, the offset distance from the central axis plays a significant role in an engines torque generation. The β -Stirlocharger has a crank radius of 0.5cm as compared to the α -Stirlocharger's crank radius of 2cm. Therefore, inherently the α engine will produce a larger torque.

The α -engine incorporates a swivel joint at the flywheel connection. This joint helps in accounting for manufacturing tolerance errors and minimizes any sticking that takes places due to friction. Another design feature to minimize friction and

manufacturing errors due to tolerancing is the rotational freedom of the cylinder mounting brackets. As the two pistons reciprocate an uneven thrust is produced due to the forces produced while in motion. These forces push the piston against the cylinder wall which creates a strong frictional force between the two surfaces and can cause sticking if the manufacturing tolerances are not tight. To minimize this friction, keeping the cylinder mounting brackets free to rotate in 1 degree of freedom significantly enhances the reciprocating motion.

In comparison to current production turbochargers and superchargers the stirlocharger is significantly lighter in weight. As a stirling engine replaces the turbine within a turbocharger to form the Stirlocharger, a fair comparison can only be made with the weight of the turbine. The turbine of the IHI turbocharger installed on the Yanmar engine in the test lab weighs 10lbm. The α and β stirling engines weigh 2lbm and 1lbm respectively. Even though these are prototype engines not designed for robustness and durability the weight reduction is approximately 9lbm and 8lbm when using the β and α versions of the Stirlocharger respectively. This is a significant reduction in weight when correlated with the overall vehicle gross weight. Every 125lbs of weight decrease increases the overall efficiency of the vehicle by 0.5mpg (Davis, 1991). This is equivalent to 0.004mpg increase in the efficiency for every pound of weight reduction. Therefore, the α and β Stirlochargers will increase the overall vehicle efficiency by 0.036mpg and 0.032mpg respectively.

5.5.2 Performance

The performance calculations of the two Stirlocharger models are performed by solving the equations which create their theoretical background. The performance equations are derived and stated in chapter 4.

a) Power

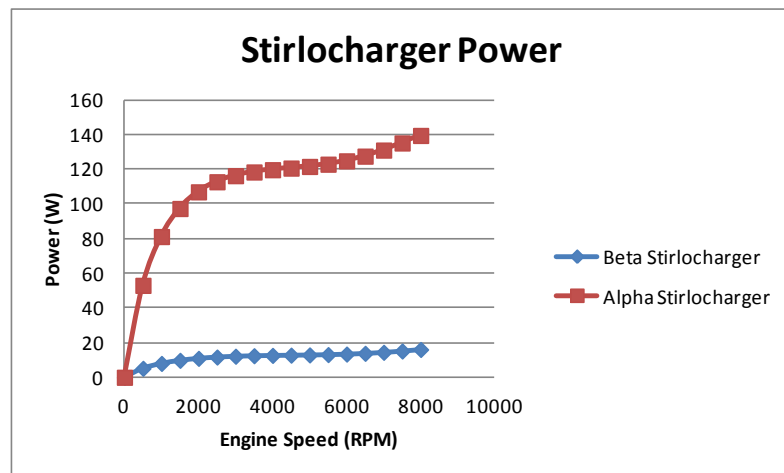
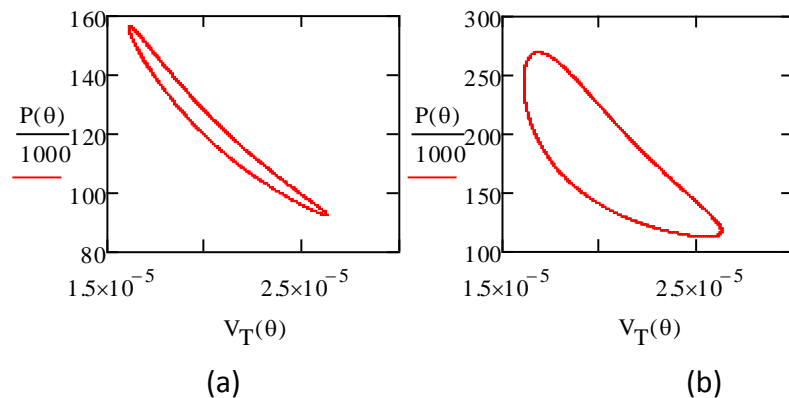


Figure 5-14: A comparison of the β and α Stirlocharger output power

The α -Stirlocharger generates a significantly larger amount of power as compared to the β engine as is shown in Fig 6.1 above. This increased power production by the α engine is due to its larger dimensions increasing its displaced volume V_D . Also due to its larger piston cylinder diameters, it has a higher surface area for exhaust heat absorption through convection. This increased heat absorption increases its work output. The work has a direct correlation with the mean pressure and thus the mass of the working gas as shown in section 4.2 eq (1). As the mass of working gas increases the mean pressure also increases, increasing the total work linearly.

The work is also defined as the area enclosed by the P-V plot. The increase in work can be seen from the increase in the area enclosed within the P-V diagram. This increase in area can be seen in the P-V diagram of the α and β Stirlochargers in Fig 6.2. The work for both the Stirlochargers when the engine is running at 100 RPM is very small as can be seen by the areas displaced. This is due to the very low levels of engine exhaust mass flow rate, also the engine out temperatures are lower at lower engine speeds due to excessive heat losses through the combustion chamber into the engine block. However, when the engine speed is increased to 6000 RPM the work output significantly increases. This is due to the higher engine out exhaust mass flow rate, and higher engine out exhaust temperatures. The temperatures are greater at higher engine speeds due to faster mean piston speeds and lower time for heat transfer at TDC leading towards higher energy to remain for the next combustion cycle.



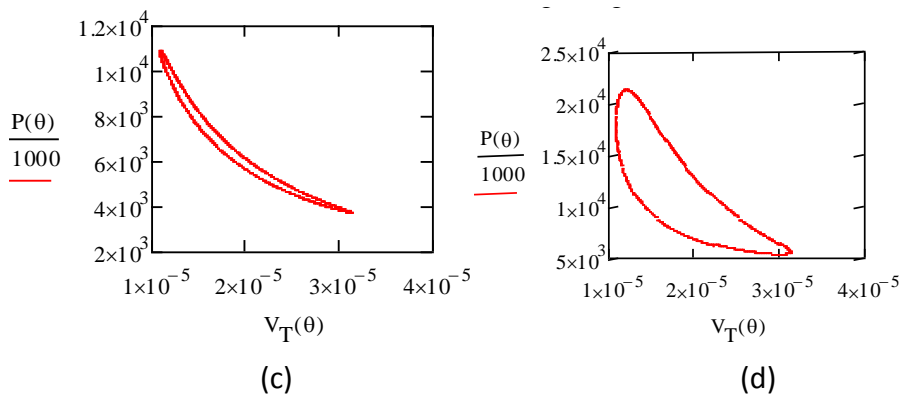


Figure 5-15: Increase in the area within the P-V diagram for the Stirlocharger. (a) P-V diagram for β -Stirlocharger at engine speed 100 RPM, (b) P-V diagram for β -Stirlocharger at engine speed 6000 RPM, (c) P-V diagram for α -Stirlocharger at engine speed 100 RPM, (d) P-V diagram for α -Stirlocharger at engine speed 6000 RPM

b) Stirlocharger Speed

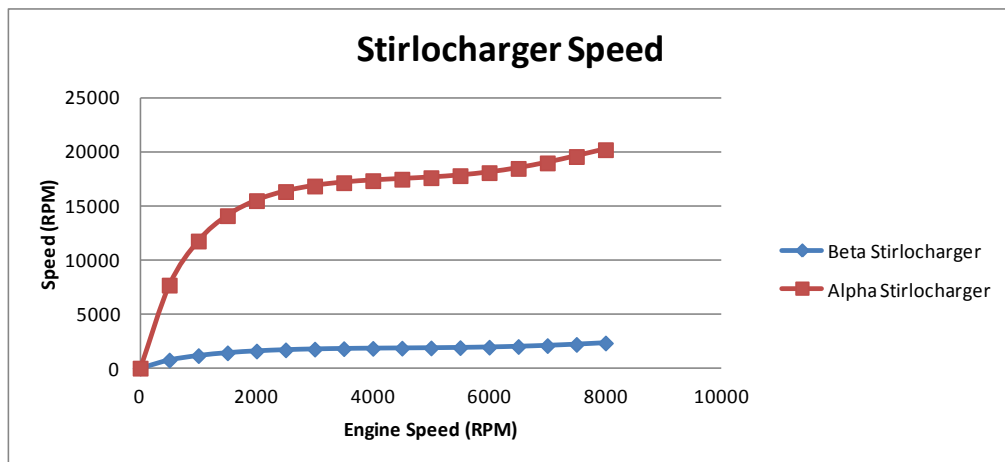


Figure 5-16: Comparison between the Speed of the Stirlocharger for α and β engines.

The speed of the Stirlocharger is dependant of the work output. The higher the work output the higher the speed of the Stirlocharger will be. The relationship between the speed, torque and power is,

$$N(rpm) = \frac{P(kW) * 9549}{T(Nm)}$$

To calculate the speed of the stirlocharger, the input power is the Stirling engine power output, and the torque is the torque required to spin the compressor impeller which was measured and is described in section 7.2.

Here we see a similar relationship between the α and β engines and is shown in Fig 6.3.

Due to the higher power output of the α -Stirlocharger it can attain higher speeds.

c) Generated Boost Pressure

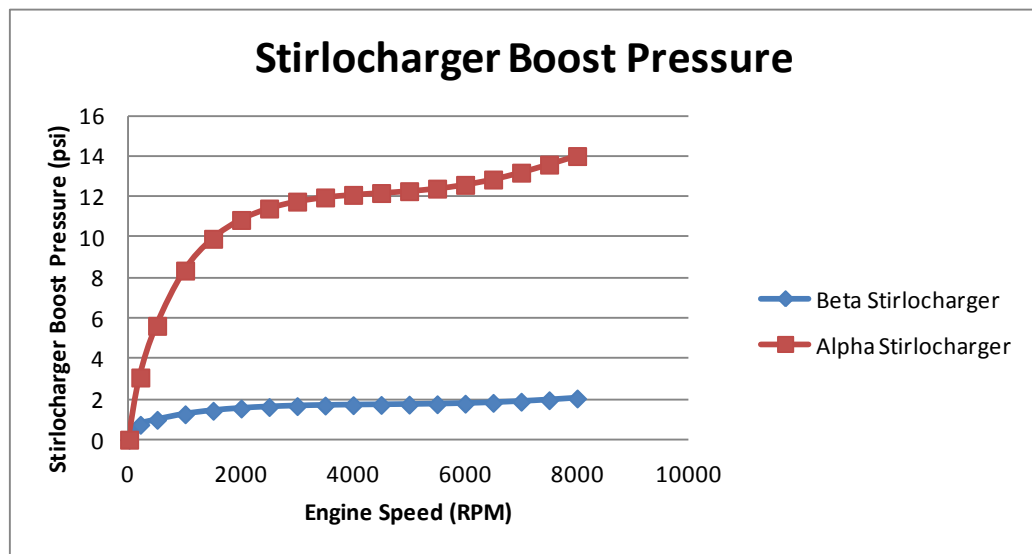


Figure 5-17: Comparison of the boost pressure generated by the α and β engines

The Stirlocharger boost pressure is dependent on the pressure ratio created by the compressor across the inlet and outlet. The boost pressure is calculated using equations described in section 4.4. Due to the higher work output and therefore higher speeds, the α -Stirlocharger shows greater boost pressures than the β -Stirlocharger. The boost pressures generated by the α engine are slightly low as compared to the turbochargers that are currently in production, however at higher engine speeds they

can be compared to current turbochargers. The compressor map for the IHI RHF4 compressor used is shown in Fig 6.5. The figure also shows the peak and average delta pressure for the α -Stirlocharger at engine speeds of 8000 RPM and 2300 RPM respectively. The α engine's boost pressure is significantly lower than these values.

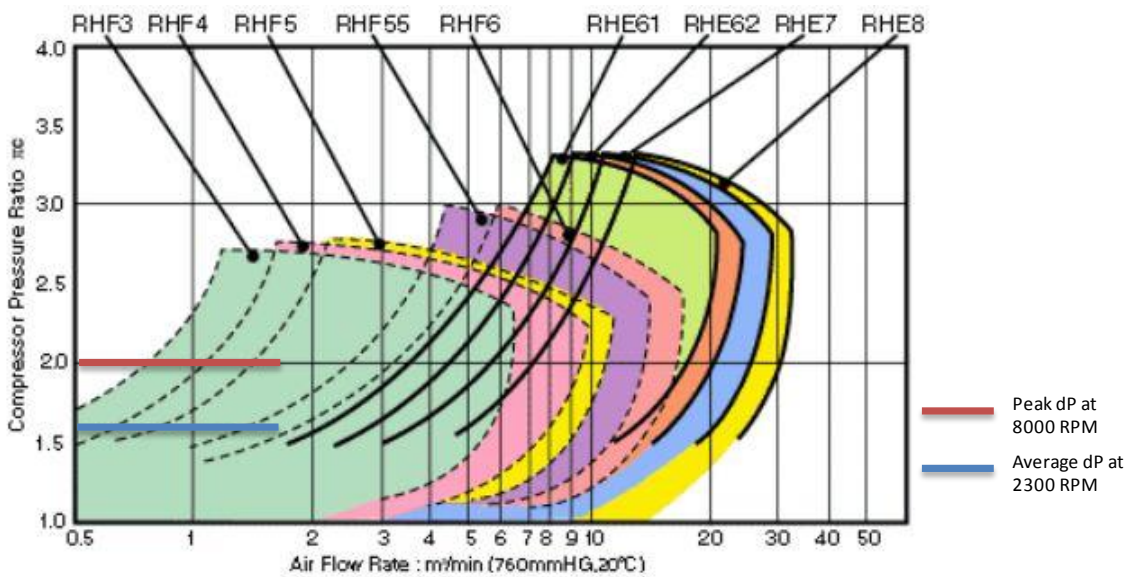


Figure 5-18: IHI RHF4 Compressor Map showing the peak and average dP produced by the α -Stirlocharger

d) Stirlocharger Mass Flow Rate

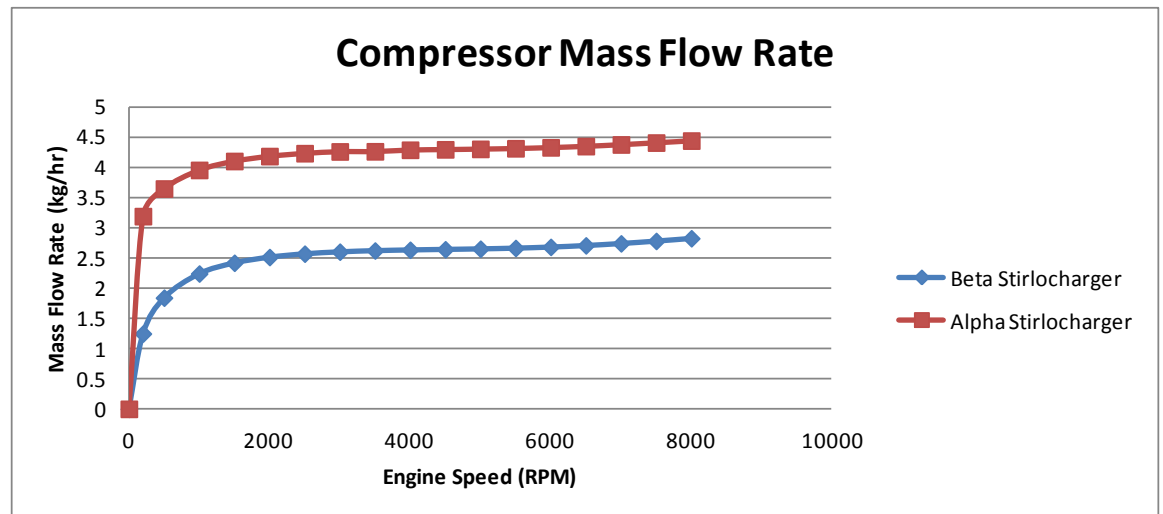


Figure 5-19: A comparison of the α and β Stirlocharger compressor mass flow rates.

The mass flow rates are almost twice as higher for the α -Stirlocharger as compared to the β . The mass flow rates are dependent on the work output of the stirlochargers, and therefore follow a similar trend. For this simulation a compressor efficiency (η_C) was chosen to be 75% with a mechanical efficiency (η_M) of 75%. The choice of these values is based on average compressor and mechanical efficiencies described by Schafer, 2012.

e) Thermal Efficiency

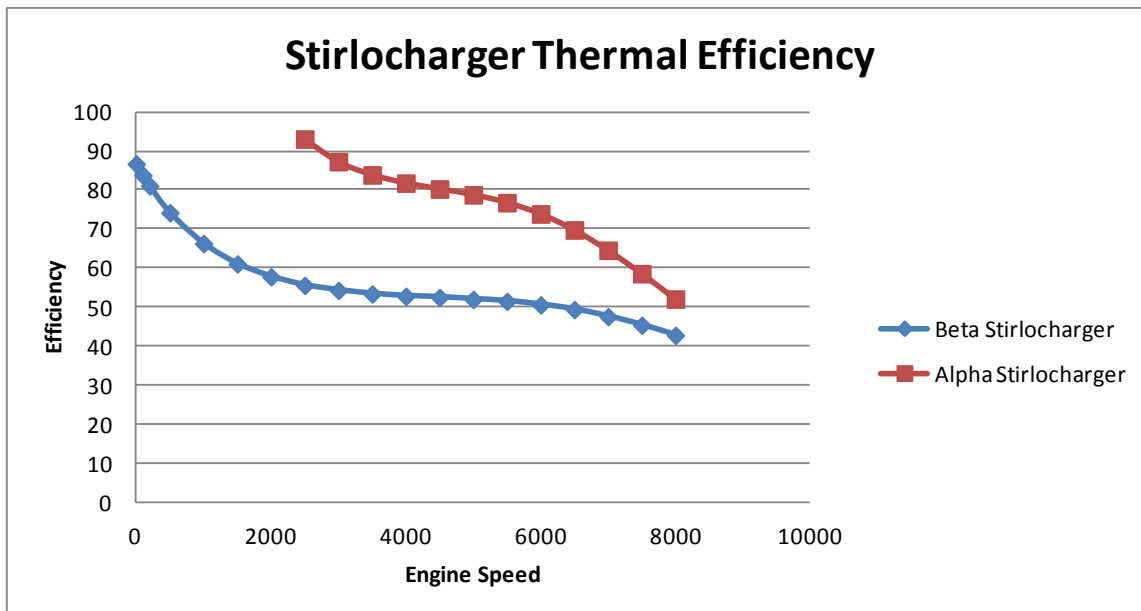


Figure 5-20: A comparison of the thermal efficiencies between the α and β Stirlochargers.

The thermal efficiency of the Stirlocharger is based on the convective heat transfer input to the hot space by the engine out exhaust gas. The efficiencies for the α and β Stirlochargers are shown in Fig 6.7. The efficiencies drop as the engine speed is increased due to higher exhaust velocities. The higher exhaust velocities provide lesser heat transfer time to the hot side of the Stirlocharger leading to a drop in thermal efficiency. The efficiency of the α -Stirlocharger drops at a steeper rate than the β . The slope of the power curve for the α engine is steeper than the β engine, therefore the efficiency drop for the α is also steeper than the β engine.

f) Engine Indicated Work

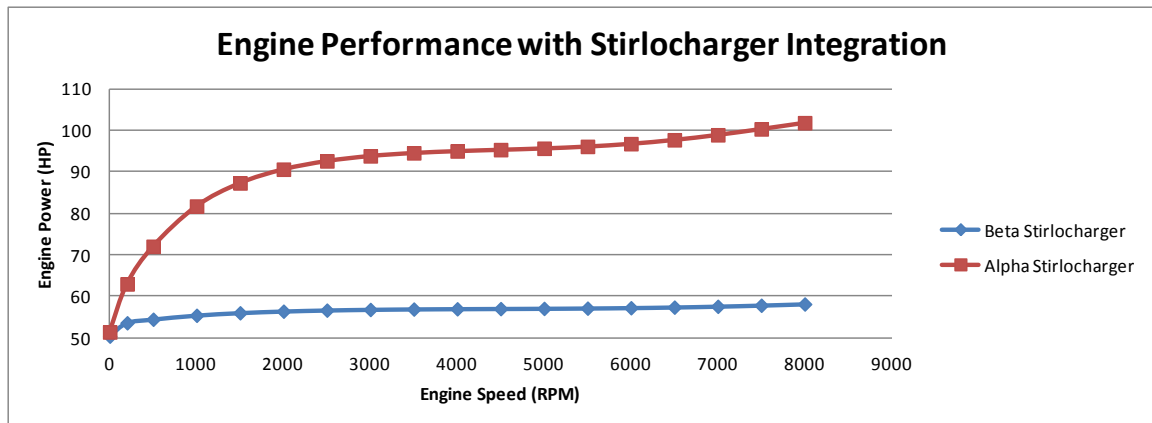


Figure 5-21: Comparison of the affect on engine performance between the α and β engine

The performance increase of the 2L Yanmar diesel engine was calculated using the standard adiabatic equations for internal combustion engines. The base engine power output is 50HP at 3000rpm. The α -Stirlocharger has increased this power output to 95hp at 3000 rpm, for ideal conditions.

The response time of the Stirlocharger is 90 sec at 1000 engine RPM, and 154.73 sec at 8000 engine RPM.

5.5.3 CONCLUSION

The Stirlocharger, a concept of waste heat recovery utilizing a stirling engine to convert heat energy into torque to power a compressor, can be a viable option for current on-highway and off-highway automotive applications. After a preliminary analysis of the two Stirlocharger models, the α -type Stirlocharger is comparable to current turbochargers in terms of performance and efficiency. The power rating of the Stirlocharger is low, however, the there is no waste gate to control the power output and therefore the Stirlocharger will be producing maximum power at all engine speeds,

the wasted exhaust energy is minimized as compared to conventional waste gate turbochargers.

Under normal operating conditions a car driver requires the most torque while overcoming a standstill vehicle, in other words while accelerating from a stop sign or a traffic intersection. Under these conditions, at full throttle, the waste gate of a conventional turbocharger is at wide open to provide maximum exhaust flow into the turbine. As the torque request from the vehicle driver is reduced the waste gate closes gradually, and lets most of the exhaust gas by-pass the turbine and out the tailpipe. This wastage also occurs while the vehicle is cruising down a highway and torque request is not very high. The Stirlocharger captures all this wasted heat and converts it into energy which is stored. Looking at Fig 6.7 the α and β Stirlocharger peak efficiencies are between the engine speeds of 3000rpm to 4500rpm and 1500rpm to 2000rpm respectively. These windows of engine speeds is what is usually seen on highway driving and off highway vehicles which run on steady duty cycles. The Stirlocharger runs optimally during these operating windows which is significant for utilizing a Stirlocharger in comparison to a conventional turbocharger.

The α -Stirlocharger produces power in the range of 100W - 120W for engine speeds between 2000rpm to 4500rpm. When the stirlocharger is used this power production is constant and is not restricted by a waste gated exhaust flow. This makes the stirlocharger generate power at all times without any restrictions and influences from the driver of the vehicle.

The α engine attains a maximum speed of 18,065 when the engine is at 6000 rpm. This speed is very low compared to the operating range of the current turbochargers of 120,000 - 180,000 rpm. Therefore, the Stirlocharger must be coupled to a gear box which can raise the speed. The α -Stirocharger is coupled with a 10:1 gear ratio, raising its peak speed at 6000 rpm to 180,654rpm which is more reasonable. Due to their nature, planetary gear trains have frictional losses of around 5% per stage. Considering this loss, the output speed of the sun gear will be reduced to 171,621rpm. After all the simulations of the Stirlocharger equations, its applicability, on a preliminary basis, to the automotive vehicles can be justified. However, more analysis needs to be done to fully understand the viability of using a Stirlocharger for automotive applications.

5.6 Recommendations

This analysis of the Stirlocharger is creating a foundation for future work to assess the viability of using Stirlochargers for automotive, aerospace and marine applications. Additional work which will make this foundation stronger are:

1. Creating an experimental basis to the Stirlocharger which can be compared with the mathematical model to validate the governing equations.
2. Considering the affects of Stirling engine losses due to mechanical inefficiencies.
3. Considering Rhombic drive Stirling engines which are known to be more efficient.
4. Incorporating second and third order design methods to these equations to increase the accuracy of the current Stirlocharger model.

5. Increasing the accuracy of the heat transfer between the exhaust gas and the hot zone of the stirling engine to get more accurate efficiency values.

LIST OF REFERENCES

LIST OF REFERENCES

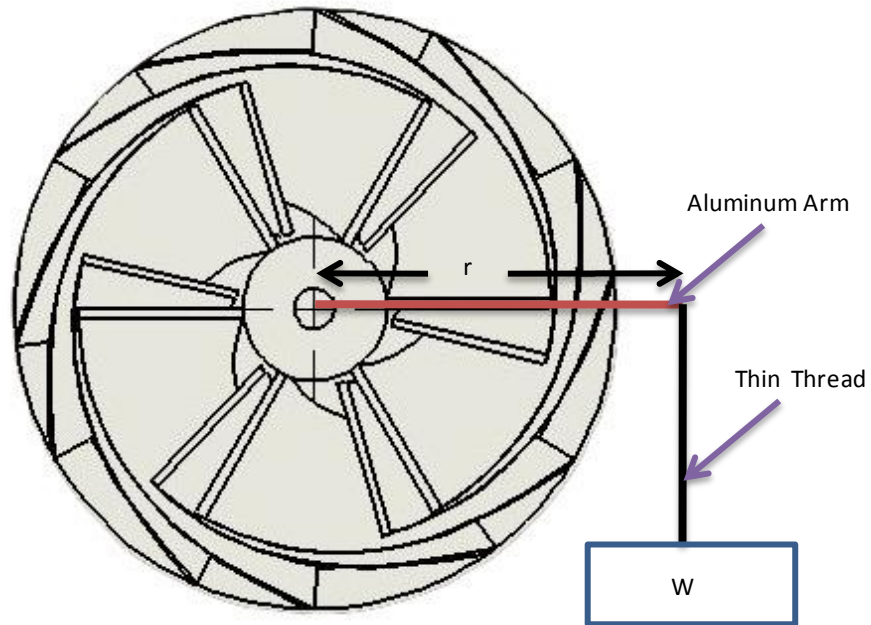
- Aghaali, H., Angstrom, H. (2013). *Temperature estimation of turbocharger working fluids and walls under different engine loads and heat transfer conditions*. SAE international.
- Cheng, C., Yang, H., Keong, L. (2013). *Theoretical and experimental study of a 300W beta-type Stirling engine*. Journal of Energy, 590 - 599.
- Gorel, A., Voss, K. (2001). *Low-pressure EGR in combination with soot filters for diesel NOx and particulate control*. SAE International, Symposium on International Automotive Technology, 153-163.
- Gu, Z., Sato, H., Feng, X. (2001) *Using supercritical heat recovery process in Stirling engines for high thermal efficiency*. Journal of applied thermal engineering, 1621 - 1630.
- Heywood, J. B. (1988). *Internal Combustion Engine Fundamentals*, McGrawHill.
- Isshiki, N., Kojima, H., Ushiyama, I., Isshiki, S. (1999). *Proposal and basic experiments of super Stirling engine*. SAE technical Papers, 34th Intersociety Energy Conversion Engineering Conference.
- Invernizzi, C. (2010). *Stirling engines using working fluids with strong real gas effects*. Journal of Applied Thermal Engineering, 1703 - 1710.

- Karabulut, H., Cinar, C., Ozturk, E., Yucesu, H. (2009). *Torque and power characteristics of a helium charged Stirling engine with a lever controlled displacer driving mechanism.* Journal of Renewable Energy, 138 - 143.
- Karabulut, H., Yucesu, H., Cinar, C., Aksoy, F. (2010). *An experimental study on the development of a β -type Stirling engine for low and moderate temperature heat sources.* Journal of Applied Energy, 68-73.
- Kongtragool, B., Wongwiset, S. (2006). *Performance of low-temperature differential Stirling engines.* Journal of Renewable Energy, 547 - 566.
- Patton, R., Bennett, G. (2011). *High efficiency internal combustion Stirling engine development.* SAE International.
- Rammal, H., Abom, M., (2007). *Acoustics of Turbochargers.* SAE International, Noise and vibration conference and exhibition.
- Sripakorn, A., Srikam, C. (2010). *Design and performance of a moderate temperature difference Stirling engine.* Journal of Renewable energy, 1728-1733.
- Serrano, J., Olmeda, P., Tiseira, A., Miguel, L., Lefebvre, A. (2013). *Theoretical and experimental study of mechanical losses in automotive turbochargers.* Journal of Energy, 888-898.
- Thombare, D.G., Verma, S.K. (2006). *Technological development in the Stirling cycle engines.* Renewable and Sustainable energy reviews, 1-38.
- Turbochargers, <http://www.turbochargers.com/>
- Scollo, L., Valdez, P., Baron, J. (2008). *Design and construction of a Stirling engine prototype.* International Journal of Hydrogen Energy, 3506 – 3510

Schafer, H (2012). Rotordynamics of Automotive Turbochargers. *Linear and Nonlinear Rotordynamics-Bearing Design-Rotor Balancing*. Springer

APPENDIX

APPENDIX

5.7 Compressor Impellor Torque Test

Trial 1

$$r = 2.8\text{cm} = 0.028\text{m}$$

$$W = 0.015\text{lbm} = 0.06672\text{N}$$

$$T = r * W = (0.028\text{m}) * (0.06672\text{N}) = 0.001868\text{N} - \text{m}$$

Trial 2

$$r = 1.6\text{cm} = 0.016\text{m}$$

$$W = 0.015\text{lbm} = 0.06672\text{N}$$

$$T = r * W = (0.016\text{m}) * (0.06672\text{N}) = 0.00106752\text{N} - \text{m}$$

Trial 3

$$r = 2.4\text{cm} = 0.024\text{m}$$

$$W = 0.015\text{lbm} = 0.06672\text{N}$$

$$T = r * W = (0.024\text{m}) * (0.06672\text{N}) = 0.06672\text{N} - \text{m}$$

5.8 Turbine Backpressure Test Data

5.8.1 Without Compressor: Air Velocity and Pressure

No.	Without Compressor: Air Velocity (ft/min)	Without Compressor: Pressure (inh2o)
1	5610	4.97
2	5590	5.034
3	5565	5.023
4	5590	5.048
5	5610	5.054
6	5535	5.049
7	5590	5.099
8	5600	5.095
9	5575	5.099
10	5565	5.115
11	5505	5.139
12	5520	5.142
13	5540	5.135
14	5485	5.143
15	5545	5.16
16	5540	5.154
17	5510	5.166
18	5520	5.131
19	5535	5.135

20	5520	5.15
21	5540	5.146
22	5500	5.137
23	5585	5.123
24	5485	5.132
25	5480	5.126
26	5490	5.141
27	5515	5.136
28	5535	5.115
29	5450	5.108
30	5470	5.107
31	5505	5.098
32	5545	5.104
33	5475	5.073
34	5465	5.083
35	5445	5.056
36	5485	5.054
37	5485	5.036
Average	5527	5.103

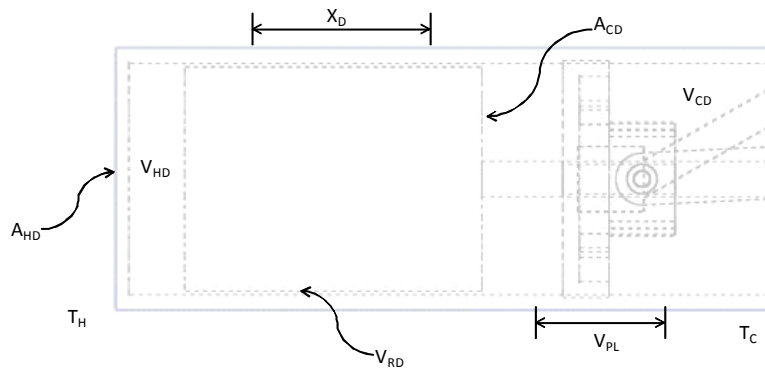
5.8.2 With Compressor: Air Velocity and Pressure

No.	With Compressor: Air Velocity (ft/min)	With Compressor: Pressure (inh2o)
1	5535	5.134
2	5480	5.159
3	5400	5.17
4	5410	5.186
5	5355	5.163
6	5365	5.151
7	5310	5.174
8	5290	5.206
9	5265	5.189
10	5305	5.198
11	5285	5.204
12	5275	5.183
13	5315	5.206
14	5285	5.19
15	5280	5.182
16	5245	5.176

17	5270	5.167
18	5245	5.155
19	5250	5.166
20	5205	5.159
21	5255	5.189
22	5215	5.157
23	5270	5.162
24	5255	5.179
25	5225	5.155
26	5265	5.158
27	5225	5.137
28	5240	5.131
29	5265	5.146
30	5215	5.135
31	5235	5.169
32	5230	5.154
33	5225	5.142
34	5180	5.136
35	5210	5.141
36	5235	5.12
37	5180	5.121
Average	5278	5.164

5.9 Simulation Code

5.9.1 β -Stirlocharger



Hot Dead Volume

$$D_B := 3.6\text{cm}$$

$$V_{HD} := \pi \left(\frac{D_B}{2} \right)^2 \cdot X = 1.018 \cdot \text{cm}^3$$

Area of Hot Face of the displacer

$$D_D := D_B - 2\text{mm}$$

$$A_{HD} := \pi \cdot \left(\frac{D_D}{2} \right)^2 = 9.079 \cdot \text{cm}^2$$

Stroke of Displacer

$$X_D := 1\text{cm}$$

Regenerator Dead Volume

$$L_D := 4.5\text{cm}$$

$$V_{RD} := \left[\pi \cdot \left(\frac{D_B}{2} \right)^2 \cdot L_D \right] - \left[\pi \cdot \left(\frac{D_D}{2} \right)^2 \cdot L_D \right] = 4.948 \cdot \text{cm}^3$$

Cold Dead Volume

$$X_{\text{Coldspace}} := 1\text{mm}$$

$$V_{CD} := \pi \cdot \left(\frac{D_B}{2} \right)^2 \cdot X_{\text{Coldspace}} = \bullet \cdot \text{cm}^3$$

$$V := 2.282 \cdot 10^{-5} \text{ m}^3$$

$$P := 101300 \text{ Pa}$$

$$R := 287 \frac{\text{J}}{\text{kg} \cdot \text{K}}$$

$$T := 300 \text{ K}$$

$$M := \frac{P \cdot V}{R \cdot T} = 0.027 \text{ gm}$$

Engine RPM --> Combustion --> Engine out temp --> Th of Stirling Engine --> Wout of Stirling Engine --> RPM --> Compressor RPM --> Boost Pressure

$$N_{\text{engine}} := 200$$

$$T_{\text{Hk}} := \left(6 \cdot 10^{-9} \cdot N_{\text{engine}}^3 \right) - \left(8 \cdot 10^{-5} \cdot N_{\text{engine}}^2 + (0.3775 \cdot N_{\text{engine}}) \right) + 40.173$$

$$T_{\text{Hk}} := -1 \cdot 10^{-5} \cdot N_{\text{engine}}^2 + 0.1778 \cdot N_{\text{engine}} + 194.41$$

$$T_{\text{H}} := (T_{\text{Hk}} + 273) \text{ K}$$

$$T_{\text{H}} = 385.521 \text{ K}$$

Area of Cold face of the Displacer

$$A_{CD} := A_{HD} = 9.079 \cdot \text{cm}^2$$

Power Piston Live Volume

$$D_P := D_B \quad X_P := 1 \text{ cm}$$

$$V_{PL} := \pi \cdot \left(\frac{D_P}{2} \right)^2 \cdot X_P = 10.179 \cdot \text{cm}^3$$

Cold Gas Temperature

$$T_C := 300 \text{ K}$$

Gas Inventory

$$M := 0.027 \text{ gm}$$

$$R := 287 \frac{\text{J}}{\text{kg} \cdot \text{K}}$$

$$P := 101300 \text{ Pa}$$

$$\alpha := 90 \text{ deg}$$

$$V_{HL} := A_{HD} \cdot X_D = 9.079 \cdot \text{cm}^3$$

$$V_{CL} := A_{CD} \cdot X_D = 9.079 \cdot \text{cm}^3$$

Hot Volume

$$V_H(\theta) := \left[\frac{V_{HL}}{2} \cdot (1 - \cos(\theta)) + V_{HD} \right]$$

Cold Volume

$$V_C(\theta) := \left[\frac{V_{CL}}{2} \cdot (1 + \cos(\theta)) + V_{CD} + \frac{V_{PL}}{2} \cdot (1 - \cos(\theta - \alpha)) \right]$$

Total Volume

$$V_T(\theta) := V_H(\theta) + V_C(\theta) + V_{RD}$$

Engine Pressure

$$T_R := \frac{T_H + T_C}{2} = 342.76 \text{ K}$$

$$P(\theta) := \frac{M \cdot R}{\left(\frac{V_H(\theta)}{T_H} + \frac{V_C(\theta)}{T_C} + \frac{V_{RD}}{T_R} \right)}$$

Senft Equation for Power

$$\omega := 2 \cdot \pi$$

$$V_E := V_{HL}$$

$$V_O := V_{PL}$$

$$V_M := V_{HL} + V_{RD} + \frac{V_{PL}}{2}$$

$$\Delta T := T_H - T_C$$

$$V_C := \frac{V_{RD}}{2} + \frac{V_{CL}}{2} + \frac{V_{PL}}{2} = 12.103 \cdot \text{cm}^3$$

$$P_{\text{mean}} := \frac{M \cdot R}{\frac{V_{HL}}{2 \cdot T_H} + \frac{V_{RD}}{T_R} + \frac{V_{PL}}{2 \cdot T_C} + \frac{V_{PL}}{2 \cdot T_C}} = 128.849 \cdot \text{kPa}$$

$$W := \frac{P_{\text{mean}} \cdot \omega}{8} \cdot \frac{V_E \cdot V_O}{V_M} \cdot \frac{\Delta T \cdot \sin(90)}{T_C + \frac{V_C}{V_M} \cdot \Delta T} = 0.106 \text{ J per cycle}$$

$$W_P := W \cdot 25 = 2.64 \text{ J}$$

Speed of Compressor Impellor with Stirling engine Work Output

$$\text{Torque} := .066 \text{ N}\cdot\text{m}$$

$$\underline{N} := \frac{\frac{W_P}{1000} \cdot 9549}{\text{Torque}} = 382.019$$

$$N_{\text{rpm}} := N \cdot \text{rpm}$$

Compressor Head Calculation

$$D_{\text{impeller}} := 1 \text{ in} \quad g = 32.174 \cdot \frac{\text{ft}}{\text{sec}^2} \quad SG_{\text{air}} := 0.0013$$

$$V_{\text{peripheral}} := N_{\text{rpm}} \cdot D_{\text{impeller}} = 3.334 \cdot \frac{\text{ft}}{\text{s}}$$

$$\underline{H} := \frac{V_{\text{peripheral}}^2}{2 \cdot g} = 0.173 \cdot \text{ft}$$

$$P_{\text{pump}} := 0.433 \cdot H \cdot SG_{\text{air}} = 2.963 \times 10^{-5} \text{ m}$$

RPM vs dP Compressor

$$P_{\text{in}} := 100 \text{ kPa}$$

$$V_{\text{flowcomp}} := 5 \cdot 10^{-5} \cdot N = 0.019$$

$$dP := 0.9244 \cdot V_{\text{flowcomp}} + 1.0331 = 1.051$$

$$P_{\text{Boost}} := (dP \cdot P_{\text{in}}) - 100 \text{ kPa} = 0.736 \cdot \text{psi}$$

$$k := 0.0759 \frac{\text{W}}{\text{m}\cdot\text{K}} \quad V_{\text{exh}} := 1 \frac{\text{m}}{\text{s}} \quad P_{\text{r}} := .720$$

$$c_{\text{v}} := 718 \frac{\text{J}}{\text{kg}\cdot\text{K}} \quad D_{\text{B}} = 3.6 \cdot \text{cm} \quad D_{\text{out}} := D_{\text{B}} + 2 \text{mm} \quad \nu := 15.8 \cdot 10^{-5} \frac{\text{m}^2}{\text{s}}$$

$$\text{Re} := \frac{V_{\text{exh}} \cdot D_{\text{out}}}{\nu} = 240.506$$

$$A := 2 \cdot \pi \cdot \left(\frac{D_{\text{B}} + 2.5 \text{mm}}{2} \right) \cdot 2 \text{cm}$$

$$\text{Nu} := 0.683 \cdot \text{Re}^{0.466} \cdot P_{\text{r}}^{\frac{1}{3}} = 7.879$$

$$h := \frac{k}{D_{\text{out}}} \cdot \text{Nu} = 15.737 \frac{\text{kg}}{\text{K}\cdot\text{s}^3}$$

$$Q_{\text{conv}} := h \cdot A \cdot (T_{\text{H}} - T_{\text{C}}) = 3.256 \text{ W}$$

Stirlocharger compressor mass flow rate

$$\eta_{\text{c}} := 0.75 \quad \eta_{\text{m}} := 0.75$$

$$m_{\text{c}} := \frac{W_{\text{P}} \cdot \eta_{\text{c}} \cdot \eta_{\text{m}}}{R \cdot T_{\text{in}} \cdot \frac{k}{k-1} \cdot (dP^{\frac{k}{k-1}} - 1)} = 0.0003462 \frac{\text{kg}}{\text{s}}$$

Stirlocharger thermal efficiency

$$\eta_{\text{stirlo}} := \frac{W_{\text{P}}}{Q_{\text{conv}}} = 0.811$$

Engine Performance Calculations

$$T_1 := 325\text{K}$$

$$P_1 := P_{\text{Boost}} + 101.3\text{kPa} = 106.376\text{kPa}$$

$$P_1 := 100\text{kPa}$$

$$r_c := 15$$

$$\eta_m := 0.86$$

$$\eta_a := 0.98$$

$$\eta_v := 1.1$$

Clearance Volume

$$V_c := \frac{V_d}{r_c - 1} = 3.561 \times 10^{-5} \cdot \text{m}^3$$

State 1

$$V_1 := V_d + V_c = 0.534\text{L}$$

$$m_m := \frac{P_1 \cdot V_1}{R \cdot T_1} = 6.091 \times 10^{-4} \text{kg}$$

$$\gamma := 1.4$$

$$Q_{\text{HV}} := 45500000 \frac{\text{J}}{\text{kg}}$$

$$S := 90\text{mm}$$

$$B := 84\text{mm}$$

$$V_d := 3.14 \cdot \left(\frac{B}{2}\right)^2 \cdot S = 0.499\text{L}$$

$$\text{AF} := 37$$

$$\rho_a := 1.177 \frac{\text{kg}}{\text{m}^3}$$

State 2

$$P_2 := P_1 \cdot r_c^\gamma = 4713.789 \cdot \text{kPa}$$

$$T_2 := T_1 \cdot r_c^{\gamma-1} = 960.108 \text{ K}$$

State 3

$$m_a := \frac{AF}{AF + 1} \cdot \eta_v \cdot m_m = 6.524 \times 10^{-4} \text{ kg}$$

$$m_f := \frac{1}{AF + 1} \cdot \eta_v \cdot m_m = 1.763 \times 10^{-5} \text{ kg}$$

$$T_3 := \frac{m_f \cdot Q_{HV} \cdot \eta_c}{m_m \cdot c_v} + T_2 = 2757.828 \text{ K}$$

$$P_3 := P_2 \cdot \frac{T_3}{T_2} = 13539.962 \cdot \text{kPa}$$

State 4

$$T_4 := T_3 \cdot \left(\frac{1}{r_c}\right)^{\gamma-1} = 933.535 \text{ K}$$

$$P_4 := P_3 \cdot \left(\frac{1}{r_c}\right)^{\gamma} = 305.555 \cdot \text{kPa}$$

Work

$$\text{Work}_{34} := \frac{m_m \cdot R \cdot (T_4 - T_3)}{1 - \gamma} = 797.311 \text{ J}$$

$$\text{Work}_{12} := \frac{m_m \cdot R \cdot (T_2 - T_1)}{1 - \gamma} = -277.575 \text{ J}$$

$$W_{\text{net}} := \text{Work}_{12} + \text{Work}_{34} = 519.736 \text{ J}$$

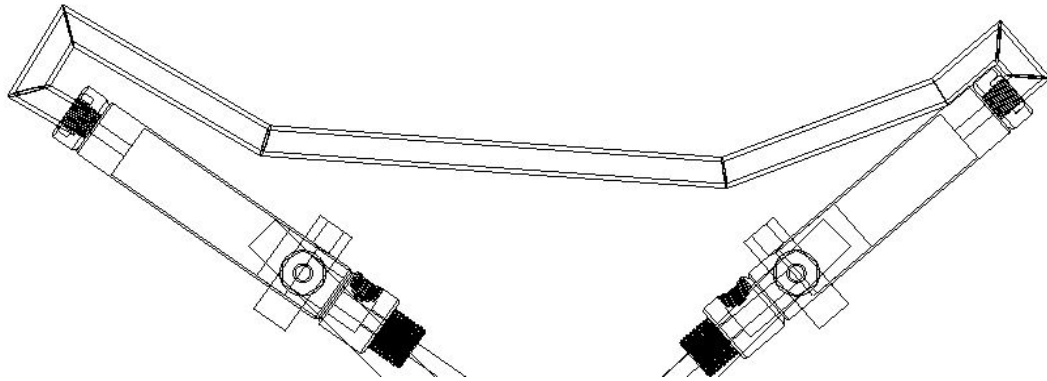
Heat in

$$Q_{\text{in}} := m_f \cdot Q_{\text{HV}} \cdot \eta_c = 786.245 \text{ J}$$

$$\eta_t := \frac{W_{\text{net}}}{Q_{\text{in}}} = 0.661$$

$$\text{imep} := \frac{W_{\text{net}}}{(V_d + V_c) - V_c} = 1042.586 \cdot \text{kPa}$$

$$W_i := \frac{W_{\text{net}} \cdot 3000 \text{ rpm}}{4} = 54.74 \cdot \text{hp}$$

5.9.2 α -Stirlocharger

Hot Volume

$$D_B := 0.75 \text{ in}$$

$$X_{\text{stroke}} := 2 \text{ in}$$

$$V_{\text{HL}} := \pi \left(\frac{D_B}{2} \right)^2 \cdot X_{\text{stroke}} = 14.479 \cdot \text{cm}^3$$

$$V_{\text{HD}} := \pi \cdot \left(\frac{D_B}{2} \right)^2 \cdot 2 \text{ mm} = 0.57 \cdot \text{cm}^3$$

$$V_{\text{H}}(\theta) := \frac{V_{\text{HL}}}{2} \cdot (1 - \sin(\theta)) + V_{\text{HD}}$$

$$D_{\text{Regen}} := 0.29 \text{ in}$$

$$V_{\text{RD}} := \pi \cdot \left(\frac{D_{\text{Regen}}}{2} \right)^2 \cdot 5 \text{ in}$$

Cold Volume

$$V_{\text{CL}} := V_{\text{HL}}$$

$$V_{\text{CD}} := V_{\text{HD}}$$

$$V_{\text{C}}(\theta) := \frac{V_{\text{CL}}}{2} \cdot (1 - \sin(\theta - 90 \text{ deg})) + V_{\text{CD}}$$

Total Volume

$$V_{\text{T}}(\theta) := V_{\text{H}}(\theta) + V_{\text{C}}(\theta) + V_{\text{RD}}$$

Engine Pressure

$$M := 1.265\text{gm}$$

$$R := 287 \frac{\text{J}}{\text{kg}\cdot\text{K}}$$

$$T_C := 300\text{K}$$

$$T_R := \frac{T_C + T_H}{2}$$

$$P(\theta) := \frac{M \cdot R}{\frac{V_H(\theta)}{T_H} + \frac{V_C(\theta)}{T_C} + \frac{V_{RD}}{T_R}}$$

Work Per Cycle

$$T_D := T_R$$

$$T_E := T_H$$

$$\tau := \frac{T_H}{T_C} = 4.284$$

$$V_E := V_{HL}$$

$$V_C := V_{CL}$$

$$k := \frac{V_C}{V_E}$$

$$P_{\max} := 1300 \text{ kPa}$$

$$\theta := \text{atan}\left(\frac{k \cdot \sin(90)}{\tau + k \cdot \cos(90)}\right) = 0.229$$

$$V_D := V_{HD} + V_{RD} + V_{CD}$$

$$X := \frac{V_D}{V_E}$$

$$S := \frac{2 \cdot X \cdot \tau}{\tau + 1}$$

$$\delta := \frac{(\tau^2 + 2 \cdot \tau \cdot k \cdot \cos(90) + k^2)^{0.5}}{\tau + k + 2 \cdot S}$$

$$W := P_{\max} \cdot V_T(\theta) \cdot \pi \cdot \frac{\tau - 1}{k + 1} \cdot \left(\frac{1 - \delta}{1 + \delta}\right)^{0.5} \cdot \frac{\delta \cdot \sin(\theta)}{1 + (1 + \delta^2)^{0.5}} = 5.581 \text{ J}$$

$$W_P := W \cdot 25 = 139.526 \text{ J}$$

Carnot Eff

$$\eta_c := 1 - \frac{T_C}{T_H} = 0.767$$

$$D_{\text{out}} := D_{\text{B}} + 2\text{mm}$$

$$P_{\text{r}} := .720$$

$$c_{\text{v}} := 718 \frac{\text{J}}{\text{kg} \cdot \text{K}}$$

$$D_{\text{B}} = 1.905 \cdot \text{cm}$$

$$V_{\text{exh}} := 3 \frac{\text{m}}{\text{s}}$$

$$k := 0.0759 \frac{\text{W}}{\text{m} \cdot \text{K}}$$

$$\text{Re} := \frac{V_{\text{exh}} \cdot D_{\text{out}}}{\nu} = 399.684$$

$$\nu := 15.8 \cdot 10^{-5} \frac{\text{m}^2}{\text{s}}$$

$$A := 2 \cdot \pi \left(\frac{D_{\text{B}} + 2.5\text{mm}}{2} \right) \cdot 2\text{cm}$$

$$\text{Nu} := 0.683 \cdot \text{Re}^{0.466} \cdot P_{\text{r}}^{\frac{1}{3}} = 9.983$$

$$h := \frac{k}{D_{\text{out}}} \cdot \text{Nu} = 200.895 \frac{\text{kg}}{\text{K} \cdot \text{s}^2}$$

$$Q_{\text{conv}} := h \cdot A \cdot (T_{\text{H}} - T_{\text{C}}) = 267.984 \text{ J}$$

Stirlocharger compressor mass flow rate

$$T_{\text{in}} := 300\text{K} \quad \eta_{\text{m}} := 0.75 \quad \eta_{\text{c}} := 0.75$$

$$m_{\text{c}} := \frac{W_{\text{P}} \cdot \eta_{\text{c}} \cdot \eta_{\text{m}}}{\left(\frac{k-1}{k} \right) \cdot R \cdot T_{\text{in}} \cdot \frac{k}{k-1} \cdot (dP^{\frac{k}{k-1}} - 1)} = 0.0012336 \text{ kg}$$

Stirlocharger thermal efficiency

$$\eta_{\text{stirlo}} := \frac{W_{\text{P}}}{Q_{\text{conv}}} = 0.521$$